Dense shelf-water and associated sediment transport in the Cap de Creus Canyon and adjacent shelf under mild winter regimes: insights from the 2021-2022 winter

- 4 Marta Arjona-Camas ^{1,2,*}, Xavier Durrieu de Madron², François Bourrin², Helena Fos¹, Anna Sanchez-
- 5 Vidal¹, David Amblas¹

1

2

3

9

10

11

12

13

14

15

16

17 18

19

20

21

22

23

24

25

26

27

28

29

30

31

32

33

34

- 6 ¹GRC Geociències Marines, Departament de Dinàmica de la Terra i de l'Oceà, Universitat de Barcelona, Barcelona, Spain.
- ²CEFREM, UMR-5110 CNRS-Université de Perpignan Via Domitia, Perpignan, France.
- 8 Correspondence to: Marta Arjona-Camas (marjona@ub.edu)

Abstract. Dense shelf water cascading (DSWC) is a key oceanographic process in transferring energy and matter from continental shelves to deep ocean areas, yet its dynamics under mild winter regimes remain poorly characterized. This study examines investigates shelf-slope transports of dense dense shelf waters and suspended particulate matter in the Cap de Creus Canyon (northwestern Mediterranean) water cascading (DSWC) and estimates the dense shelf-water and associated sediment transport in the Cap de Creus Canyon (northwestern Mediterranean) during the mild winter of 2021-2022. Observations from the The-FARDWO-CCC1 multiplatform cruise survey in March 2022 revealed the presence of dense shelf waters on the continental shelf, which were transported to the canyon head. These cold, dense, and turbid waters, rich in dissolved oxygen and chlorophyll-a, downwelled along the canyon's southern flank to <u>depths around 350-390</u> m depth. Estimated water and suspended sediment transports during this event were 0.3 Sv and 105 metric tons, During the observed downwelling event, estimated water and suspended sediment transport within the dense water vein were 0.3 Sv and 10^s metric tons, respectively, mainly confined to the upper canyon-reaches. Mid-canyon transports were lower (0.05 Sv and 10⁴, respectively), suggesting that during mild winters, dense waters either remain on the shelf, flow along the coast, or cascade only to the upper section of the Cap de Creus Canyon. These transports were low compared to extreme winters, likely due to the influence of freshwater inputs and moderate meteorological winter conditions. Transport magnitudes were higher in the upper canyon section than in the mid-canyon section, where transport was estimated at 0.05 Sv, including around 10⁴ metric tons of sediment. This observation suggests that during mild winters, while most of the dense water either remains on the shelf or the shelf edge area, or flows southward along the coast, the Cap de Creus Canyon acts only as a partial sink for cascading waters. The Mediterranean Sea Physics reanalysis data showed indicate that the cascading season lasted from late-January to mid-March 2022, approximately three months, from January to early April 2022, with several shallow cascading pulses, peaking in mid-March during an easterly/southeasterly storm. Our results show that significant export of dense shelf water (260 km³) and suspended sediment can within the canyon. The highest dense shelf water transport occurred in mid-March, associated with easterly/south-easterly windstorms. This study confirms that remarkable dense shelf water and sediment transport occur s-in the Cap de Creus Canyon under more moderate atmospheric forcings and shallow cascading. , particularly along its southern flank, even during mild winters in absence of deep cascading and limited external forcing. Nevertheless, this phenomenon mild DSWC events likely appears to make a significant contribution to the formation of the Western Intermediate Water (WIW) body in the canyon. in the region.

35

36

37

38

39

- **Keywords:** dense shelf water cascading; Western Intermediate Water; mild winter; sediment transport; <u>reanalysis;</u> Gulf of Lion; Mediterranean Sea.
- 1. Introduction
- Continental margins are dynamic transition zones that connect the are crucial transitional areas that link the terrestrial and ocean systems, and play a key role in the transfer and redistribution of particulate material (to the deeper ocean (Nittrouer

et al., 2009; Levin and Sibuet, 2012). These regions often receive substantial significant inputs of sediment, particulate material, mainly of especially from rivers and atmospheric deposition fluvial and atmospheric origin in mid-latitude margins, which accumulate into extensive deposits on the continental shelf (Blair and Aller, 2012; Liu et al., 2016; Kwon et al., 2021). While much of this material accumulates on the continental shelf, However, these inputs can be reworked and partially exported to deeper areas of the ocean by various hydrodynamic processes, such as storm waves, river floods, or ocean currents, can resuspend and transport sediments towards the continental slope and deeper areas of the ocean -(Walsh and Nittrouer, 2009). These processes include river floods that transfer large quantities of suspended sediments to the margin, and high energy storm waves that resuspend sediment from the shallower regions of the shelf. Both mechanisms can transport elevated amounts of suspended particulate matter (SPM) into deeper areas of the slope, often through submarine canyons, as turbidity eurrents or hyperpycnal flows (; Puig et al., 2014).

One particularly efficient mechanism of shelf-to-slope exchanges is dense shelf water cascading (DSWC). DSWC is a seasonal oceanographic phenomenon that occurs in marine regions worldwide. DSWC starts when surface waters over the continental shelf become denser than surrounding waters by cooling, evaporation, or sea-ice formation with brine rejection (e.g., Ivanov et al., 2004; Durrieu de Madron et al., 2005; Canals et al., 2006; Amblas and Dowdeswell, 2018; Mahjabin et al., 2019, 2020; Gales et al., 2021). Dense shelf waters then sink, generating near-bottom gravity flows that move downslope, frequently funneled through submarine canyons (Allen and Durrieu de Madron, 2009). This process contributes to the ventilation of the deep ocean, and plays an important role in the global thermohaline circulation. Additionally, it modifies the seabed along its path by eroding and depositing sediments, and facilitates the transfer of energy and matter (including sediment particles, organic carbon, pollutants, and litter) from shallow to deep waters (Canals et al., 2006; Tubau et al., 2013; Puig, 2017; Amblas and Dowdeswell, 2018).

The Gulf of Lion (GoL), located in the northwestern Mediterranean, is a very interesting region to study DSWC and for the study of shelf-slope exchanges. This region, as it receives important inputs from riverine discharge and atmospheric deposition, both rivers and atmospheric deposition (Durrieu de Madron et al., 2008) and is subject to intense physical forcing (Durrieu de Madron et al., 2008). Episodic events, such as storms or DSWC, efficiently contribute to the export of shelf waters and sediments Moreover, it is a very dynamic area where strong physical forcing prevails and where episodic events, such as storms or dense shelf water cascading (DSWC), contribute to the efficient export of shelf water and sediment towards the open sea and deeper parts of the basin (Millot, 1990; Canals et al., 2006; Palanques et al., 2006, 2008; Ogston et al., 2008). The formation of dense waters in the GoL is essentially occurs in winter, triggered by related to atmospheric forcing and occurs in winter by heat loss and evaporation induced by active and persistent (more than > 30 consecutive days) northerly and northwesterly winds (locally named Tramontane and Mistral) that induce surface heat loss, evaporation, . This results in cooling, vertical mixing, and the subsequent densification of shelf waters waters over the GoL's shelf (Durrieu de Madron et al., 2005, 2008; Canals et al., 2006). These dense waters sink until reaching their equilibrium depth and propagate along the western coast of the GoL (Fig. 1). The combined effect of the prevailing preferential cyclonic coastal circulation of coastal currents and the , combined with the narrowing of the continental shelf near the Cap de Creus Peninsula (Fig. 1), concentrates most of this dense water at the southwestern end of the gulfGoL, where it is mainly exported cause most of the export from the shelf mainly through the Lacaze-Duthiers and Cap de Creus canyons (Ulses et al., 2008); Palanques et al., 2008). In these canyons, dense waters There, dense shelf waters overspill the shelf edge and cascade down the slope (Béthoux et al., 2002; Durrieu de Madron et al., 2005), contributing to the ventilation of intermediate and deep layers. As they descend, these overflows reshape and deep waters and altering the geomorphology of the seabed along its path by eroding and depositing sediments, and promote the downslope transport of organic matter accumulated on the shelf. Ultimately, DSWC in the GoL has been observed to impact. It can also transport organic matter accumulated on the shelf to the slope and basin, and ultimately impact

84 85

86

87

88

89

90

91

92

93

94

95

96

97

98

99

00

01

102

103

04

Figure 1. (a) Bathymetric map of the GoL showing the rivers discharging into the gulf and the incised submarine canyons. Black arrows depict Tramontane and Mistral winds. The grey arrow indicates the direction of the Northern Current over the study area. (b) Bathymetric map of the southwestern part of the Gulf of Lion showing the location of Lacaze-Duthiers Canyon (LDC) and Cap de Creus Canyon (CCC). Orange triangles indicate the location of buoys (POEM, Banyuls, and SOLA). The location of the re-analysis grid-points at the shelf break (RA-SB) and within the CCC (RA-C) are indicated with dark blue dots. Green dots represent the location of CTD stations carried out during the FARDWO-CCC1 cruise. Red stars mark the location of two instrumented mooring lines deployed at ~1000 m depth at the axis of LDC (LDC-1000) and CCC (CCC-1000). The solid yellow line indicates the glider section on the continental shelf adjacent to the CCC. Dashed lines correspond to the virtual transects defined using reanalysis data: dark blue and light blue lines indicate the location of the upper and mid-canyon transects, respectively, used to estimate dense water transport during winter 2021-2022; the fuchsia dashed line marks the central canyon transect used to determine the temporal evolution of cascading events over the past 26 years (1997-2022).

Due to its relative ease of access, the GoL is particularly suitable for investigating DSWC. However, because of its intermittent nature, DSWC remains difficult to observe directly and its contribution to shelf-deep ocean exchanges is challenging to quantify. Several studies conducted in the GoL have focused on the impact of intense DSWC (IDSWC) on shelf-slope exchanges. investigated the importance of extreme DSWC events on shelf-slope exchanges. These particularly intense extreme events were monitored in the winters of 1998-1999 (Heussner et al., 2006), 2004-2005 (Canals et al., 2006; Ogston et al., 2008; Puig et al., 2008), 2005-2006 (Pasqual et al., 2010; Sanchez-Vidal et al., 2008), and 2011-2012 (Durrieu de Madron et al., 2013; Palanques and Puig, 2018), with instrumented mooring lines deployed at ~1000 m depth in by instrumented mooring lines placed at depths ~ 1,000 m in Lacaze-Duthiers and Cap de Creus Canyons. One of the most studied

extreme-IDSWC events occurred events is the DSWC that occurred in the severe winter of 2004-2005. Over 40 days, more than two thirds (750 km³) of GoL's shelf waters cascaded through the Cap de Creus Canyon (Canals et al., 2006; Ulses et al., 2008b), maintaining cold temperatures (11-12.7 °C), high down-canyon velocities (> 0.8 m·s⁻¹) and high suspended sediment concentrations (30-40 mg·L⁻¹). This DSWC event also transported ~0.6·10⁶ tons of organic carbon downcanyon, a mass comparable to the mean annual solid transport of all rivers discharging into the GoL (Canals et al., 2006; Tesi et al., 2010).

Although IDSWC events have drawn particular attention due to their significant impacts, Nonetheless, moderate-mild DSWC (MDSWC) events are in fact the most common frequent since the set of the observational era in the GoL, and they are expected to become even-more prevalent under the climate change scenario (Herrmann et al., 2008; Durrieu de Madron et al., 2023). These events typically occur during mild winters, driven characterized by by quieter atmospheric conditions and lower heat losses (Martín et al., 2013; Rumín-Caparrós et al., 2013; Mikolajczak et al., 2020). During such winters, intense the cold continental winds that drive dense water formation are weaker and less persistent, typically blowing for fewer than 30 days and rarely exceeding speeds of, which are key for dense water formation, are less frequent than usual (less than 30 days) and rarely exceed speeds of 10 m·s⁻¹. In contrast, easterly and southeasterly winds become are unusually more frequent and sustained, sometimes blowing for more than three consecutive days and often blow for more than three consecutive days (Mikolajczak et al., 2020). At the same time, river discharges, Additionally, moderate to high river discharges, particularly from the Rhône River, supply freshwater to the GoL's shelf, further limiting the densification of shelf waters (Ulses et al., 2008a). As a result, most of the dense shelf waters are mixed with lighter ambient waters on the shelf before reaching the slope, and only a small fraction is exported along the coast or to the upper slope, where it contributes to the body of Western Intermediate Water (-of these foreings, the density of shelf waters remains moderate, with less buoyancy loss than in extreme events (Mikolajczak et al., 2020). Consequently, dense waters over the GoL's shelf are mainly consumed by mixing with lighter ambient waters, and only a small fraction of them escapes to deeper areas of the slope (Duffau-Juliand et al., 2004; Herrmann et al., 2008). Ulses et al. (2008a) For instance, during the mild winter of 2003-2004, Ulses et al. (2008a) estimated a total export of dense shelf waters of 75 km³ in the mild winter of 2003-2004, an order of magnitude smaller than during extreme-IDSWC events. Similarly, during the winter of 2010-2011, Another good example is the winter of 2010-2011, when only brief and shallow cascading was observed in the Cap de Creus Canyon down to 350 m depth recorded (Martín et al., 2013; Rumín-Caparrós et al., 2013). More recently, modeling studies have expanded our understanding on the interannual variability of dense water export under different atmospheric scenarios, and emphasized the role of moderate winters in driving MDSWC events in the GoL (Mikolajczak et al., 2020).

Nonetheless, most existing studies have relied on numerical simulations and time series from fixed mooring stations, which offer limited spatial resolution and lack direct observations of shelf-slope exchanges. To date, there has been no comprehensive observational characterization of dense water and sediment transport from the shelf to the slope in the Cap de Creus Canyon under moderate winter conditions during MDSWC events. To address this gap, the present study documents and characterizes MDSWC in the Cap de Creus during the winter of 2021-2022. We combine hydrographic and velocity measurements collected within the canyon and on the adjacent shelf to investigate the shelf-to-slope transport of dense waters and suspended sediment, along with reanalysis data to determine the temporal extent of this event and place it in the context of cascading events observed in the Cap de Creus Canyon over the past 26 years. By focusing on a mild winter scenario, we aim to provide insights into MDSWC events and discuss the implications for WIW formation and deep-sea ecosystems. However, and the cap de Creus Canyon during a period of low loss of buoyancy (Martín et al., 2013; Bourrin et al., 2015), capturing the downwelling of cold, low salinity, and turbid waters to 350 m depth on the canyon's southern flank (Martín et al., 2013). Numerical simulations by Mikolajezak et al. (2020) indicate that, despite contrasting atmospheric conditions, the total dense water export during the mild winter of 2010-2011 (1,500 km²) was of the same magnitude as during the extreme winter of 2004-2005 (1,640 km²) (Ulses et al.,

2008a). The key difference lay in the preferential export pathways: in winter 2010-2011, 30 % of the export occurred through the Cap de Creus Canyon, while 70 % followed along the coast. This distribution was reversed in winter 2004-2005, when 69 % of the exported dense shelf water passed through the canyon (Ulses et al., 2008a). However, the limited number of observations in the Cap de Creus Canyon during the mild winter of 2010-2011, mainly based on moored time series, constrained the full characterization of the shelf to canyon export of dense shelf waters during this moderate DSWC event.

The present study aims to comprehensively investigate the hydrographic characteristics, hydrodynamics and export routes of a mild cascading event in the Cap de Creus Canyon and its adjacent shelf during the winter of 2021–2022. This work is based on hydrographic data collected during a multiplatform survey in the Cap de Creus Canyon, which was monitored during the FARDWO CCC1 cruise, and simultaneous measurements at its adjacent shelf acquired during a glider survey as part of the MELANGE DUNES experiment. These datasets enabled us to capture the dynamics of the event over two days in March 2022 and directly quantify the export of water and suspended particulate matter. To provide a broader temporal perspective, reanalysis data were used to determine the duration of the cascading season and estimate the variability of dense shelf water export within the Cap de Creus Canyon during the mild winter of 2021–2022.

2. Study area

2.1. General setting

The GoL is a micro-tidal river-dominated continental margin that extends from the Cap Croisette Peninsula, in the northern part of the gulf, to the Cap de Creus Peninsula at its southwestern limit (Fig. 1a). It is characterized by a wide continental shelf (up to 70 km) and it is incised by a dense network of submarine canyons (Lastras et al., 2007).

The ocean circulation of the GoL is primarily driven by the Northern Current, which flows along the continental slope from the northeast to the southwest (Millot, 1990; Raimbault et al., 2003). This current is part of the cyclonic general circulation of the Western Mediterranean basin and it is especially intense during winter months (Lapouyade and Durrieu de Madron, 2001; Petrenko et al., 2008). The GoL is also impacted by strong continental winds from the north and northwest (Mistral and Tramontane, respectively), which favor dense water formation and cascading events in winter (Durrieu de Madron et al., 2013) and coastal upwellings in summer (Odic et al., 2022). Humid easterly and southeasterly winds, which blow less frequently, occur primarily from autumn to spring, and can produce large swells and high waves over the continental shelf (Ferré et al., 2005; Leredde et al., 2007; Petrenko et al., 2008; Guizien, 2009). They do not produce a densification of surface waters but lead to an intense cyclonic circulation on the GoL's shelf and to a strong export of shelf waters at the southwestern exit of the Gulf GoL (Ulses et al., 2008a; Mikolajczak et al., 2020).

The ocean circulation of the GoL is also influenced by the freshwater inputs from the Rhône River, one of the largest Mediterranean Rivers, and a series of smaller rivers with typical flash-flooding regimes (Ludwig et al., 2009). The Rhône River supplies an annual river discharge of 1,700 m³·s⁻¹ and an average of 8.4 Mt·y¹ of suspended particulate matter (Sadaoui et al., 22016; Poulier et al., 2019). The smaller rivers (from south to north the Tech, Têt, Agly, Aude, Orb, Hérault, Lez, and Vidourle) account for slightly 5% of the total inputs of particulate matter (~0.5 Mt·y⁻¹) to the GoL (Serrat et al., 2001; Bourrin et al., 2006). Most of the sediment delivered by these rivers is temporarily stored near their mouths in deltas and prodeltas (Drexler and Nittrouer, 2008), and afterwards it is remobilized and redistributed along the margin by the action of storms and the wind-driven along-shelf currents permanent Northern Current (Millot, 1990; Guillén et al., 2006; Ulses et al., 2008a; Estournel et al., 2023). This westerly current carries particulate material from the shelf towards the southwestern end of the GoL, where the continental shelf rapidly narrows and the Cap de Creus Peninsula constraints the circulation, acts as a barrier to the flow, increasing intensifying the water flow and increasing the particle concentration the concentration of water and particles (Durrieu de Madron et al., 1990; Canals et al., 2006).

The Cap de Creus Canyon represents the limit between the GoL and the Catalan margin (Fig. 1b). The canyon head is located only 4 km from the coast and incises the shelf edge at 110-130 m depth (Lastras et al., 2007). Due to its proximity to the coast and the preferential direction of coastal currents, this canyon has been identified as the main pathway for the transfer of water and sediments from the shelf to the slope and deep margin (Canals et al., 2006; Palanques et al., 2006, 2012).

2.2. Hydrography

187

188

189

190

91

92

93

94

195

196

197

198

199

200

201

202

203

204

205

206

207

208

209

210

211

212

213

214

215

216

217

218

219

220

221

222

223

224

225

226

The surface layers in over the GoL shelf stratify between late spring and autumn (Millot, 1990). In winter, the surface cooling and wind-driven mixing weaken the stratification-weakens due to the cold temperatures, which leads to a vertically homogeneous and the water column becomes homogeneous over the continental shelf (Durrieu de Madron and Panouse, 1996). Offshore, the GoL is characterized by several water masses. The Atlantic Water (AW) fills the upper 250 m and flows into the Mediterranean Sea through the Strait of Gibraltar. During its transit to the GoL, its hydrographic properties undergo chemical and physical modifications, becoming the "old" Atlantic Water (oAW) with T > 13 °C and S = 38.0-38.2 (Millot, 1999). Below, the Eastern Intermediate Water (EIW) occupies the water column between 250 and 850 m depth. It is formed during winter in the Levantine Basin, in the Eastern Mediterranean Sea, by intermediate convection (Font, 1987; Millot, 1999; Taillandier et al., 2022; Schroeder et al., 2024). The Western Mediterranean Deep Water (WMDW) occupies the deepest bathymetric levels and is formed in winter at interannual scales in the GoL by open-ocean deep convection. It typically shows $T \sim 13$ °C and S = 13 °C and S38.43-38.47 (Marshall and Schott, 1999; Somot et al., 2016). During winter, northerly and north-westerly Mistral and Tramontane winds cause the formation of dense shelf waters (DSW) over the GoL's shelf (T < 13 °C and S < 38.4) (Houpert et al., 2016; Testor et al., 2018). During mild winters, these dense waters do not gain enough density ($\sigma < 29.05 \text{ kg} \cdot \text{m}^{-3}$) to sink into the deep basin, and contribute to DSW can be detached at intermediate depths and contribute to the Western Intermediate Water (WIW) (T = 12.6-13.0 °C and S = 38.1-38.3) body body, which is found at upper slope depths (\sim 350-380-400 m) (Dufau-Julliand et al., 2004; Durrieu de Madron et al., 2005; Juza et al., 2013). This occasionally happens in autumn or during mild winters, when the downwelling of DSW is limited to 300 400 m depth by stratification. The formation of WIW is an important process in the Mediterranean Thermohaline Circulation (MTHC), as it contributes to the ventilation of intermediate layers and plays a role in preconditioning the region for deeper convection events (Juza et al., 2019). During the coldest extreme winters, the potential excess density of DSW gain exceeds that of the EIW ($\sigma = 29.05-29.10 \text{ kg} \cdot \text{m}^{-3}$) and even surpasses the density of the WMDW ($\sigma = 29.10-29.16 \text{ kg/m}^3$), enabling DSWC to allows DSW to reach the deep basin around 2000-2500 m depth. This process contributes, and contributes to the ventilation of the deep waters and to the final characteristics of the WMDW (Durrieu de Madron, 2013; Palanques and Puig, 2018).

3. Materials and methods

3.1. Field data acquisition

3.1.1. Hydrographic transects and current vertical profiles

During the FARDWO-CCC1 Cruise, onboard the R/V *García del Cid*, two hydrographic transects were conducted on March 5-6, 2022, across the Cap de Creus Canyon, with stations spaced every 1.5 km (Fig. 1b). The T1 transect covered the upper section of the canyon, while the T2 transect covered the mid-canyon section. The hydrographic data were collected using a SeaBird 9 CTD probe coupled with a SeaPoint Fluorometer and Turbidity Sensor (700 nm), an SBE43 dissolved oxygen sensor, and a WetLabs C-Star Transmissometer (650 nm). These sensors were mounted on a rosette system with twelve 12 L Niskin bottles, which collected water samples from various depths. The CTD-Rosette system was hauled through the water column, allowing the comparison of sensor outputs in productive surface waters with high fluorescence, in clear midwaters, and in intermediate and bottom nepheloid layers loaded with fine suspended particulate matter. Potential temperature, practical salinity, and potential density were calculated using the state of the seawater TEOS 10 equation (Feistel, 2003; 2008). The hydrographic profiles obtained from the CTD stations were interpolated onto a regular grid using the isopycnic gridding

229 230

237 238 239

240

241

242

243

244

236

268

269

method. This method is an advance gridding procedure that aligns property contours along lines of constant potential density (isopycnals) rather than constant depth, which improves the representation of water mass structure and reduces artificial smoothing across density gradients (Schlitzer, 2022).

Velocity profiles were simultaneously measured using two Lowered Acoustic Doppler Current Profiler (LADCPs) Teledyne 300 kHz narrowband units mounted on the CTD frame. One unit faced upwards and the other downwards to maximize the total range of velocity observations. Each instrument was configured with 20 bins, each 8 m in length, which allowed for a measurement range of ~160 m (Thurnherr, 2010). The raw LADCP data were processed using the LDEO Software version IX by applying the least-squared method, using the navigation and the vessel-mounted (VM) ADCP data as constraints (Visbeck, 2002).

3.1.2. Vessel-mounted (VM) ADCP data

The R/V García del Cid was equipped with a vessel-mounted (VM) 75 kHz ADCP (Ocean Surveyor, RD Instruments) that recorded current velocities along the hydrographic sections. The VM-ADCP was configured to record current velocities at 2-min averages, while sampling depths were set to 8-m vertical bins. The VM-ADCP data were processed using the CASCADE V7.2 software (Le Bot et al., 2011). Absolute current velocities resulted from removing the vessel speed, derived from a differential global positioning system. The measurement range of the instrument was from 20 m to 720 m depth. Given the micro-tidal regime of the Mediterranean Sea (tidal range ~ 0.5 m), tides are considered of very low magnitude in the GoL (Davis and Hayes, 1984; Dipper, 2022). Nevertheless, a barotropic tide correction was applied to the VM-ADCP data using the OTIS-TPX8 Tide model (https://www.tpxo.net/global) within the cascade V7.2 software, which provided tide-corrected current velocities. VM-ADCP data were then screened to align with the timeframe of the different hydrographic sections. However, the VM-ADCP's range could not fully cover the water column due to the interaction of secondary acoustical lobes with the seabed. To address this limitation, we integrated VM-ADCP data with LADCP measurements recorded at each station. This integration involved aligning time stamps, matching coordinate systems, and merging and interpolating datasets.

Finally, ADCP velocities, decomposed into E-W and N-S components, were rotated 15° counterclockwise to align with the local canyon axis orientation. This rotation provided the across- and along-canyon velocity components for interpretation. For the across-canyon component, eastward velocities have been defined as positive and westward velocities as negative. For the along-canyon component, up-canyon velocities are positive, while down-canyon velocities are negative.

3.1.3. Glider observations

The hydrodynamics of dense shelf waters at the southwestern tip of the continental shelf adjacent to the Cap de Creus Canyon were monitored by a SeaExplorer underwater glider (ALSEAMAR-ALCEN). The glider carried out one along-shelf (i.e., north-south) section and navigated 10 km for 25 hours, starting on March 5, 2022 (Fig. 1b). It conducted a total of 28 yos (down/up casts). It followed a sawtooth-shaped trajectory through the water column, descending typically to 2 m above the bottom (between 83 and 92 m depth) and ascending to 0-1 m of distance from the surface. The glider was equipped with a pumped SeaBird GPCTD, coupled with a dissolved oxygen sensor (SBE43F), that acquired temperature, conductivity, and pressure data at a sampling rate of 4s. Salinity, potential temperature, and potential density were derived using the TEOS 10 equation (Feistel, 2003; 2008). Additionally, the glider had a SeaBird Triplet (WetLabs FLBBCD sensor), which measured proxies of phytoplankton abundance (by measuring the fluorescence of chlorophyll-a at 470/695 nm), and total particle concentration (by measuring optical backscattering at 700 nm). Finally, the glider integrated a downward-looking AD2CP (Acoustic Doppler Dual Current Profiler) that measured relative water column velocities and the glider speed. The AD2CP was configured with 15 vertically stacked cells of 2 m resolution, and a sampling frequency of 5 s. Raw velocity measurements were processed using the shear method to derive absolute current velocities (Fischer and Visbeck, 1993; Thurnherr et al., 2015; Homrani et al., 2025). We used bottom tracking and GPS coordinates as constraints to reference each velocity profile.

The hydrographic profiles obtained from the glider were similarly interpolated using the isopycnic gridding method as applied to the CTD data (Schlitzer, 2022).

3.2. Ancillary data

.

\$00

\$01

\$03

\$04

3.2.1. Environmental forcings and shelf observational data

Heat flux data were used to evaluate the interaction between the atmosphere and the ocean surface. Data were retrieved from the European Centre for Middle-range Forecast (ECMWF) ERA5 reanalysis by Copernicus Climate Change Service. This global reanalysis product provides hourly estimates of a large number of atmospheric variables since 1940, with a horizontal resolution of 0.25 ° (Hersbach et al., 2023). For this study, the sea-atmosphere interactions were assessed from 42.6 °N to 43.4 °N and from 3 °E to 4.5 °E, approximately covering the entire GoL's continental shelf, from October 2021 to July 2022.

Significant wave height (Hs) data were retrieved from the Banyuls buoy (06601) located at 42.49 °N and 3.17 °E (Fig. 1b), through the French CANDHIS database (https://candhis.cerema.fr). These measurements were recorded every 30 min using a directional wave buoy (Datawell DWR MkIII 70). Wind speed and direction data were obtained from the POEM buoy (https://www.seanoe.org/data/00777/88936/; Bourrin et al., 2022), which records hourly observations using a surface meteorological sensor and is also equipped with a multiparametric CTD probe measuring near-surface temperature and salinity. In addition, the SOLA station, located in the Bay of Banyuls-sur-Mer (Fig. 1) and managed by the SOMLIT network (https://www.seanoe.org/data/00886/99794/; Conan et al., 2024) provided weekly near-bottom (~27 km) time series of temperature, salinity, and pressure. This data allowed to monitor the presence of dense shelf waters over the continental shelf during the winter of 2021-2022. Raw data were processed to remove gaps and outliers prior to analysis.

Water discharge of rivers opening to the GoL was measured by gauging stations located near rivers mouths and provided by Hydro Portail v3.1.4.3 (https://hydro.eaufrance.fr). For this study, we have considered the river discharge from the Rhône River and the total discharge from coastal rivers as the sum of their individual contribution.

3.2.2. Instrumented mooring lines

3.2.3 Instrumented mooring lines

Current velocity and direction, temperature, and SPM concentration were monitored in two submarine canyons, the Lacaze-Duthiers Canyon (LDC) and the Cap de Creus Canyon (CCC)eanyons, by means of two instrumented mooring lines (Fig. 1b). The mooring line at Lacaze-Duthiers Canyon, located at about 1000 m depth, has been maintained in the canyon since 1993 as part of the MOOSE program. It is equipped with two current meters (Nortek Aquadopp 2 MHz) with temperature, conductivity, and turbidity sensors, placed at 500 m and 1,000 m depth (referred to as LDC-500 and LDC-1000, respectively). The sampling interval for the current meters was set to 60 min. The fixed mooring line at the Cap de Creus Canyon has been maintained in the canyon axis by the University of Barcelona since December 2010-2009. This mooring line, referred to as CCC-1000, is equipped with a current metter (Nortek Aquadopp 2 MHz) with temperature, conductivity, and a SeaPoint turbidity sensors placed at 18 m above the bottom (mab). The current meter sampling interval was set to 15 min. For this study, the recording period was considered from OctoberDecember 1, 2021 to April 1, 2022, which encompassed the winter of 2021-2022.period and the FARDWO-CCC1 Cruise.

3.3. Determination of suspended particulate matter (SPM) concentration from turbidity measurements

To calibrate turbidity measurements obtained in the Cap de Creus Canyon during the FARDWO-CCC1 Cruise, water samples were collected at selected depths with Niskin bottles. For each sample, between 2 and 3 L of water were vacuum filtered into 47 mm 0.4 µm pre-weighted Nucleopore filters. The filters were then rinsed with MiliQ water to remove salt and

stored at 4 °C. Then, these filters were dried by desiccation and weighted. The weighing difference of the filters divided by the volume filtered of seawater yielded to the SPM concentration, in $mg \cdot L^{-1}$. Finally, the measured SPM concentrations were plotted against in situ turbidity measurements, both from the transmissometer and the optical sensor (Figs. 2a, b). The beam attenuation coefficient (BAC) from the transmissometer showed a stronger correlation with SPM ($R^2 = 0.86$) compared to FTU from the SeaPoint turbidity sensor ($R^2 = 0.81$). Therefore, SPM concentrations were predicted using the equation:

$$SPM = 1.84 \cdot BAC + 0.05 (R^2 = 0.85; n = 25)_{(1)}$$

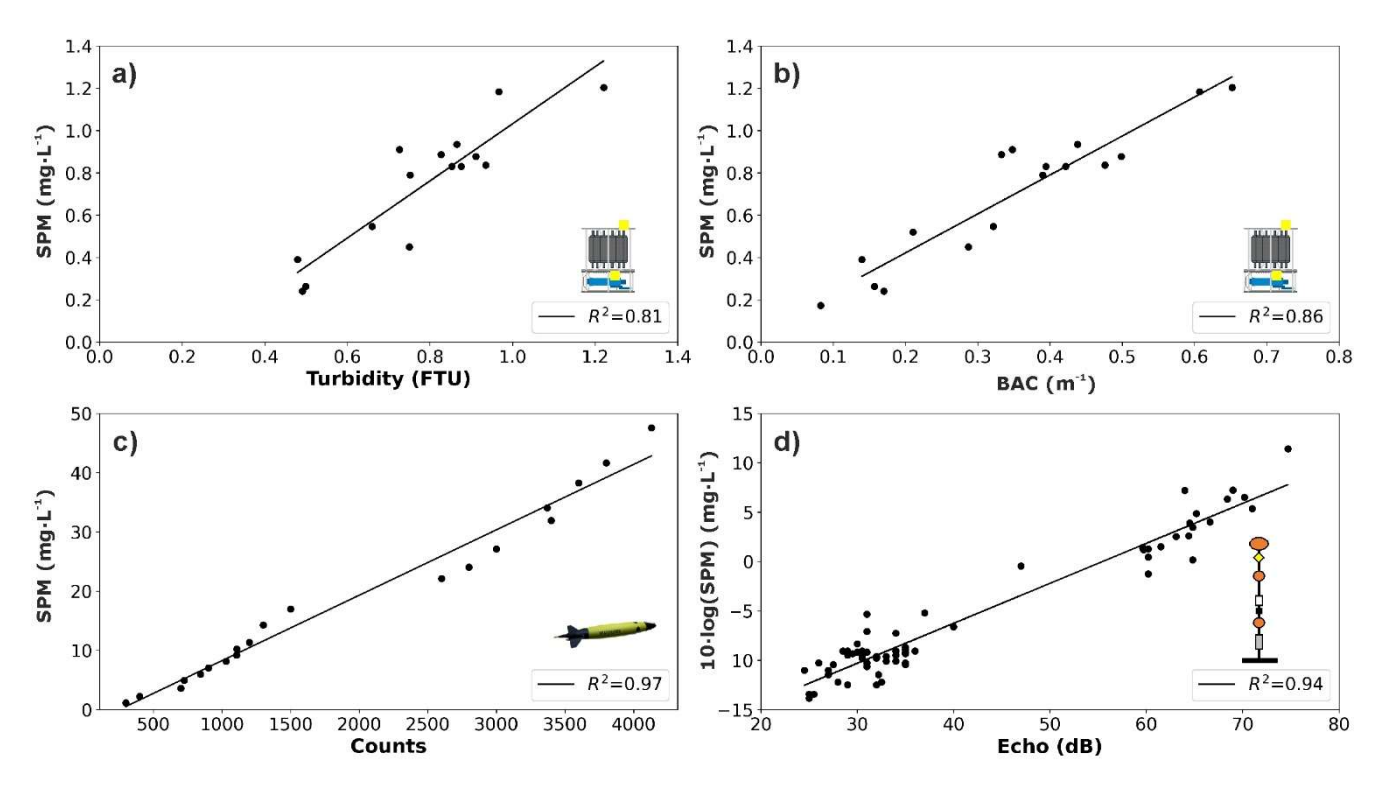


Figure 2. Relationship between the weighed SPM mass concentration (mg·L⁻¹) and: (a) turbidity records (FTU) from the SeaPoint sensor and (b) BAC (m⁻¹) from the WetLabs transmissometer attached to the CTD-rosette system; (c) optical backscatter sensor data (counts) from the WetLabs FLBBCD sensor mounted on the SeaExplorer glider; (d) echo intensity (dB) retrieved from the current meters installed in LDC and CCC instrumented moorings. For each relationship, the regression coefficient (R²) is given.

Backscatter data (in counts) from a self-contained FLBBCD optical sensor, identical to the one installed the optical sensor on the SeaExplorer glider, were also correlated to SPM concentration using a laboratory calibration. Firstly, the optical sensor was submerged into a 10-L plastic tank filled with freshwater. Then, sediment was added while stirring the water to distribute the sediment particles evenly. The amount of sediment was gradually increased until the instrument reached a saturation level of approximately 4,000 counts, corresponding to a sediment mass of 447.5 mg. The optical sensor, connected to a computer, displayed and stored the turbidity measurements during the calibration process. Then, water samples were taken at each interval and filtered, obtaining SPM concentration (in mg·L-1). Pairs of counts/SPM data points yielded the following regression line (Fig. 2c):

SPM =
$$0.01 \cdot \text{counts}$$
 (R² = 0.97 ; n = 20) (2)

Finally, echo intensity (EI) records from the current meters equipped in LDC and CCC lines were also correlated with SPM concentration, using a linear equation relating the logarithm of SPM to EI (Gartner, 2004). Unlike optical devices, acoustic sensors measure relative particle concentrations based on changes on the backscattered acoustic signal (Fugate and Friedrichs, 2002). Acoustic backscatter, expressed in counts, is proportional to the decibel sound pressure level (Lohrmann,

2001), and depends on the particle size and on the operating frequency of the acoustic sensor (Wilson and Hay, 2015). The equation derived from the regression between backscatter data and direct sampling concentration in the GoL was (Fig. 2d):

$$10 \cdot \log (SPM) = 0.405 \cdot EI - 22.46 (R^2 = 0.94; n = 66)_{(3)}$$

3.4. Estimation of dense water and SPM transports from observations

The total transports of dense shelf water and associated SPM were estimated using hydrographic and current measurements collected during the FARDWO-CCC1 cruise and the glider survey conducted in early March 2022 in the Cap de Creus Canyon and its adjacent shelf, respectively.

First, to isolate dense shelf waters, we selected water masses with a potential temperature below 12.9 °C and potential density below 29.05 kg·m⁻³. At the canyon, these properties already corresponded to the signature of the Western Intermediate Water (WIW). Then, dense water transport (expressed in $Sv = 1 \cdot 10^6 \, \text{m}^3 \cdot \text{s}^{-1}$) was calculated by integrating the zonal component of current speed (which aligns with the down-canyon direction) over the area occupied by dense waters. For the T1 and T2 transects, current speed was measured using the LADCP attached to the CTD-rosette system, and transport was calculated in vertical cells of 8 m (the LADCP bin size) and then integrated over the whole transect. For the glider section over the continental shelf, dense water transport was computed using the same approach, although current velocity data were obtained from the glider-mounted AD2CP.

After estimating dense water transport, we computed the associated SPM transport (in metric tons) by multiplying the calculated water transport by the SPM concentration within the dense water layer. SPM concentrations were derived from the SeaPoint sensor integrated into the CTD probe for the canyon transects, and from the WetLabs FLBBCD sensor onboard the glider for the shelf section. Finally, all SPM profiles were resampled to match the vertical resolution of current velocity measurements prior to integration.

3.5. Reanalysis data

\$43

\$45

\$57

\$60

\$67

\$70

To complement the observational dataset, we used the Mediterranean Sea Physics Reanalysis (hereafter MedSea) from the Copernicus Marine Service to evaluate the spatiotemporal evolution of hydrographic properties and transport patterns of dense shelf waters in the Cap de Creus Canyon. This reanalysis product has a horizontal resolution of 1/24° (~4-5 km) and provides daily estimates of ocean variables, including temperature, salinity, and currents at multiple depths (Escudier et al., 2020, 2021).

First, we used the MedSea data to assess the temporal evolution of hydrographic conditions during winter 2021-2022. Daily time series of temperature and salinity were extracted from two grid points at key locations along the pathway of dense waters: one located at the shelf break (RA-SB: 42.48 °N and 3.29 °E, depth= 250 m), and another within the Cap de Creus Canyon (RA-C: 42.34 °N and 3.37 °E, depth= 350 m) (Fig. 1b).

Then, we calculated the transport of dense shelf waters through the canyon using MedSea data by applying the same approach as for the observational dataset. First, we identified dense waters using the same hydrographic thresholds (T < 12.9 °C and σ < 29.05 kg·m⁻³). Then, we estimated the dense water transport (in Sv) by integrating the zonal velocity component (aligned with the downcanyon direction) across two virtual transects close to the T1 and T2 sections sampled during the FARDWO-CCC1 cruise. This analysis was performed for the winter of 2021-2022 to capture the temporal variability of the transport, and allowed us to extend the analysis beyond the limited period covered by the field data. Finally, to determine the temporal context and interannual variability of dense shelf water transport, we analyzed a 26-year (1997-2022) time series of MedSea reanalysis data across a central transect in the Cap de Creus Canyon (see location in Figure 1). Dense waters were identified by temperature < 12.9 °C and zonal velocity > 0 m·s⁻¹ (down-canyon velocities). We distinguished IDSWC events by a density threshold > 29.1 kg·m⁻³, whereas MDSWC events were characterized by densities below this threshold. This long-term analysis allowed us to place the 2021–2022 MDSWC event in the context of other cascading episodes previously reported in the Gulf of Lion and to evaluate its relative intensity.

4. Results

377

378

\$79

\$80

381

\$82

\$83

\$84

385

\$86

\$87

\$88

\$89

\$90

\$91

\$92

\$93

\$94

\$95

\$96

\$97

398

399

400

401

402

403

404

405

406

407

408

409

410

411

412

413

414

415

416

417

418 419

4.1 Meteorological and oceanographic conditions during winter 2021-2022

The time series of net heat fluxes from over the GoL's shelf showed negative values from July October 2021 to early October April 20221, reflecting indicating a heat loss from the ocean to the atmosphere (Fig. 3a). The strongest net heat losses during that winter occurred in November 2021 and January 2022, reaching values of about -400 W·m⁻² (Fig. 3a).

Winter 2021-2022 was characterized by frequent northerly and north_westerly winds (Tramontane and Mistral) with speeds ranging from 5 to 18 m·s⁻¹ (Fig. 3b). The duration of these wind events varied throughout winterthe season, blowing in short bursts of periods of 1 to 3 days during October and December, and in longer periods of 5 to 7 consecutive days during November and February (Fig. 3b). The highest wind speeds during this period exceeded 20 m·s⁻¹ and were associated with strong heat losses (Figs. 3b, c). From March to July May 2022, the wind pattern alternated between northerly/north-westerly winds and short intervals periods (2-4 days) of easterly/southeasterly winds (Fig. 3b). As Similar to in winter, the strongest heat losses, which occurred in April 2022, and coincided with a relatively longer long period (5 days) of northerly/north-westerly winds with relatively high speeds (>above 20 m·s⁻¹) (Figs. 3a, b).

Significant wave height (Hs) <u>ranged between</u> <u>was generally low during winter</u>, <u>ranging between</u> 0.5 and 2.0 m <u>during winter</u> (Fig. 3c). During this period, <u>only one marine storma single storm</u>, defined as sustained Hs > 2 m for more than 6 hours (Mendoza and Jimenez, 2009), was recorded on March 13, 2022. This storm was <u>associated with an eaused by a moderate</u> easterly/south-easterly wind event <u>with maximum speeds of ~ 19 m·s⁻¹, and generated and was accompanied with Hs > 3 m for <u>more overthan</u> 20 hours (Fig. 3c).</u>

The mean water discharge of the Rhône River generally displayed average values of about 1,700850 m³·s⁻¹ (Fig. 3d; Pont et al., 2002; Provansal et al., 2014). However, the discharge exceeded 2,000 m³·s⁻¹ during early October, early November, and mid-December 2021 (Fig. 3d). A peak discharge of over 5,000 m³·s⁻¹ occurred in late December, associated with a brief without any associated major storm easterly/south-easterly wind event (Fig. 3c). Coastal river discharges remained relatively low throughout winter (see average daily water discharge values in Bourrin et al., 2006) during all the time period, typically below 200 m³·s⁻¹, except for a few brief short episodes where when river discharge reached > exceeded 400 m³·s⁻¹ (Fig. 3d). The highest coastal river discharge occurred on March 13, 2022, concomitantly—after a period of sustained to an easterly/southeasterly winds event (Fig. 3c). During this event, Tthe coastal river discharges reached 2,265 m³·s⁻¹, surpassing the water discharge of the Rhône River, which was relatively comparatively smalllower (884 m³·s⁻¹) (Fig. 3d).

The near-bottom temperature time series on at the continental shelf, extracted measured from by the POEM buoy, showed a gradual decline from 20 °C in October 2021 to 13 °C in March 2022 (Fig. 3e). Salinity fluctuated between 37.8 to 38.1 during the same this period, occasionally dropping below 37.8 in parallel with temperature decreases (Fig. 3f). Near-bottom temperature and salinity time series at the shelf break (250 m depth) and at the Cap de Creus Canyon (350 m depth), as previously noted, were derived from reanalysis data. At the shelf break (250 m depth), near-bottom temperature remained constant around 14.5 °C, except for an increase to 15.5 °C throughout November and a subsequent decrease below 13 °C from January to late March 2022 (Fig. 3e). Salinity at the shelf break also remained constant (~38.55) throughout the studied winter (Fig. 3f). At the Cap de Creus Canyon, (350 m depth), temperature and salinity remained constant stable around 14.5 °C and 38.8, respectively, during winter. However, fFrom late January to late March 2022, both variables occasionally dropped in short-lived pulses to 12.9 °C and 38.1, respectively, before returning to their baseline previous values (Figs. 3e, f). The potential density anomaly at the shelf and shelf break followed the seasonal temperature variations, and it only increased during February-March 2022 when it peaked at ~28.9 kg·m⁻³ (Fig. 3g). In contrast, density at the Cap de Creus Canyon remained relatively stable, throughout the study period, slightly varying between 28.75 and 28.95 kg·m⁻³ throughout the study period (Fig. 3g).

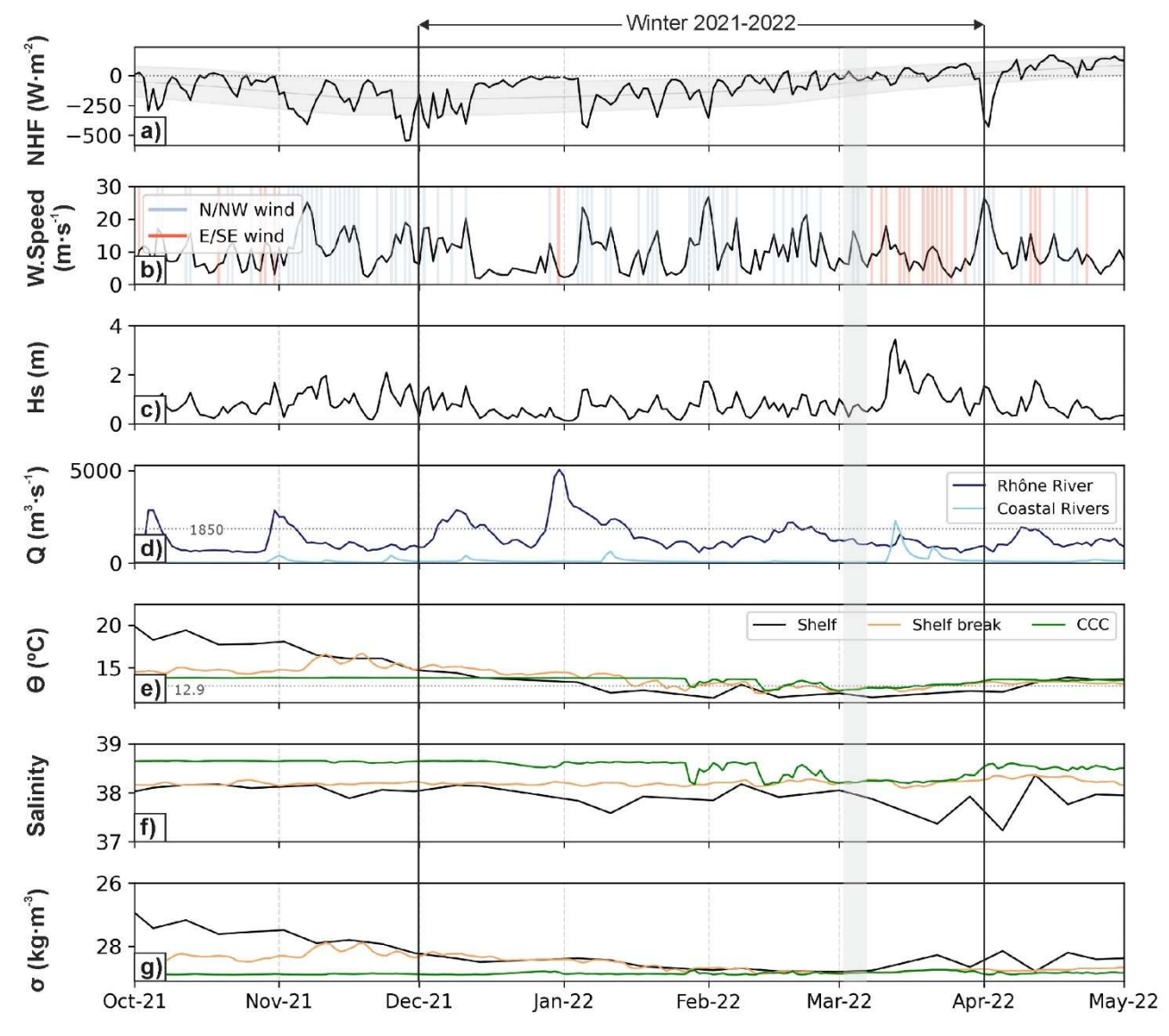


Figure 3. Time series of (a) net heat fluxes (NHF, W·m⁻²) averaged over the GoL's shelf; (b) wind speed (m·s⁻¹) measured at the POEM buoy. Blue and red shaded bars indicate N/NW and S/SE winds, respectively; (c) significant wave height (Hs, m) measured at the Banyuls buoy; (d) river discharge (Q, m³·s⁻¹) of the Rhône River (dark blue) and coastal river discharges discharging into the GoL (light blue); (e) weekly mean bottom temperature (θ, °C), (f) salinity, and (g) potential density (σ, kg·m⁻³) calculated from TS data at the continental shelf (black), the shelf break (orange), and the Cap de Creus Canyon (green). Data at the continental shelf were extracted measured atfrom the POEM buoy. Data at the shelf break and within the Cap de Creus Canyon were extracted from two grid points from the MedSeaMediterranean Sea Physics Reanalysis product. All data are displayed for the period between July-October 2021 and July-May 2022. The grey shaded vertical bar highlights the FARDWO-CCC1 Cruise, which took place on March 1-7th, 2022. The studied winter period is also The DSW formation period is markedindicated in the figure and corresponds to the period time when of most negative NHF values are negative, indicating the strongest ocean heat loss to the atmosphere and favorable conditions for enhanced DSWC events.

4.2 Time series at LDC Lacaze-Duthiers and Cap de Creus canyons and CCC during winter 2021-2022

<u>Figure 4 shows the Time-time</u> series of temperature, current speed and direction, and SPM <u>recorded at the mooring stations in Lacaze-Duthiers Canyon (at 500 and 1000 m depth) and the Cap de Creus Canyon (at 1000 m depth) <u>eoncentration at LDC-500, LDC-1000</u>, and <u>CCC-1000 mooring stations</u> during winter 2021-2022, are shown in Figure 4.</u>

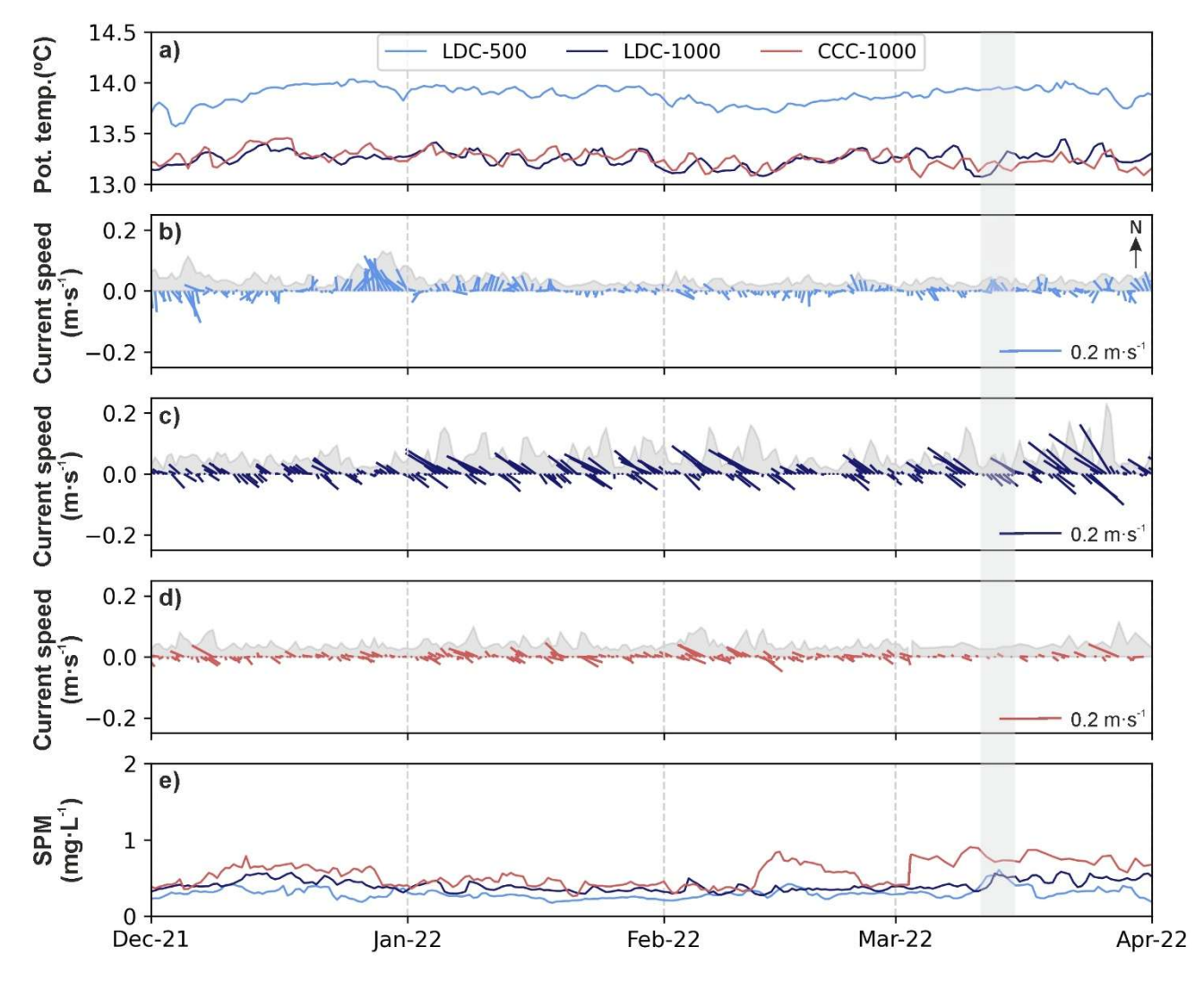


Figure 4. Time series of (a) potential temperature (°C), (b-d) stick plots of currents and current speed as a shaded grey area (m·s⁻¹), and (e) suspended particulate matter concentration (SPM, mg·L⁻¹) measured at the mooring stations in Lacaze-Duthiers Canyon (LDC-500 in (light blue, and), LDC-1000 in (dark blue), and CCCCap de Creus Canyon (CCC-1000 in (red) during winter 2021-2022 mooring stations. In panels (b-d), arrows indicate the along-canyon component for each mooring site. The grey shaded vertical bar highlights the FARDWO-CCC1 Cruise, which took place on March 1-7, 2022.

39

40

54

At 500 m depth in Lacaze-Duthiers Canyn (LDC-500), temperature remained relatively constant between 13.5 and 14 °C, whereas-while at 1000 m in both Lacaze-Duthiers and Cap de Creus canyonsat LDC-1000 and CCC-1000, it fluctuated between 13.1 and 13.4 °C (Fig. 4a). Current speeds was generally low and ranged from 0.01 to 0.1 m·s⁻¹ at LDC-500 in Lacaze-Duthiers Canyon and at 1000 m in the Cap de Creus Canyon CCC-1000 (Figs. 4b, d), and from 0.1 and 0.2 m·s⁻¹ at 1000 m in Lacaze-Duthiers Canyonslightly higher at LDC-1000, where it varied between 0.1 and 0.2 m·s⁻¹ (Fig. 4c). At this depth, LDC-1000, current speed increased several times to 0.12 m·s⁻¹ between January and mid-March 2022, and to peaked at 0.2 m·s⁻¹ in late March (Fig. 4c). A similar, but less intense peak in late March—was observed at in the Cap de Creus Canyon at 1000 m during the same period CCC-1000 (Fig. 4c), coinciding with —These increases coincided with small temperature decreases drops (Fig. 4a). Current direction at 500 m in Lacaze-Duthiers Canyon at LDC-500 was isotropic (Fig. 4b), whereas while at 1000 m in both LDCLacaze-Duthiers and Cap de Creus canyons, 1000 and CCC-1000 it was became anisotropic and preferentially—aligned with the orientation of the respective canyon axes with the axes of Lacaze-Duthiers and Cap de Creus canyons (Figs. 4c, d).

The time series of SPM concentration at all mooring sites <u>during winter 2021-2022</u> showed <u>values ranging low values</u> during <u>winter 2021-2022</u>, ranging between 0.2 and 0.5 mg·L⁻¹ at all monitored depths (Fig. 4e). The highest SPM concentrations were recorded <u>at 1000 m depth in the Cap de Creus Canyon from mid-February to late March 2022-at CCC-1000</u>, reaching values of ~ 0.51 mg·L⁻¹ (Fig. 4e).

4.3. Water column properties at the <u>Cap de Creus Canyon CCC</u> and adjacent shelf <u>in March 2022 during the FARDWO-CCC1 Cruise</u>

4.3.1. Hydrographic and biogeochemical properties

57

60

63

72

73

79

86

The continental shelf adjacent to the Cap de Creus Canyon was monitored on March 5, using a SeaExplorer glider, which monitored the continental shelf water column from the surface down to a depth of 92 m depthat the southwestern tip of the Cap de Creus Canyon. In the northern part of the shelf transect, a water mass with temperatures of 12.9 °C and salinities of 38.2 occupied most of the water column above the 28.95 kg·m⁻³ isopycnal (Figs. 5a-c). This water mass exhibited SPM concentrations of 1.5-3.0 mg·L⁻¹ and dissolved oxygen values of ~232 µmol·kg⁻¹ (Figs. 6a, c). Near the bottom, a relatively cooler, fresher, and more turbid water mass with higher dissolved oxygen concentrations was observed in the northern part of the section (Figs. 5a-c and 6a-c). This water mass flowed southward along the shelf below the 28.95 kg·m⁻³ isopycnal, gradually becoming slightly warmer, saltier, less turbid, and less oxygenated towards the southern part of the shelf transect (Figs. 5a-c and 6a-c). Fluorescence values generally increased towards the southern part of the shelf transect (Fig. 6b). These hydrographic and biogeochemical properties clearly indicate the presence of dense shelf waters on the continental shelf in the shape of a wedge that thickened towards the coast the Cap de Creus Peninsula (i.e., south) near the bottom (Figs. 5a-c and 6a-c). These results reflect the oceanographic conditions on the continental shelf shortly before the start of the FARDWO-CCC1 cruise.

During the FARDWO-CCC1 cruise, two ship-based CTD transects were conducted across the Cap de Creus Canyon. The FARDWO-CCC1-T1 Transect transect was carried out across the upper section of the canyonCap de Creus Canyon, from the surface down to a maximum depth of 625 m depth. The upper water column (< 100 m depth) was characterized by temperatures of 13-13.2 °C, salinities of ~38.25 (Figs. 5d, e), dissolved oxygen concentrations of ~200 μmol·kg⁻¹, and relatively low SPM concentrations (0.3 mg·L⁻¹) (Figs. 6d, f). Beneath this layer, a colder (12.2-12.7 °C), fresher (S = 38.1-38.2) water mass occupied depths of 100-350 400 m along the southern flank of the canyon (Fig. 5d, f). This water mass showed relatively high dissolved oxygen values (> 200 μmol·kg⁻¹) and increased SPM concentrations (1-1.2 mg·L⁻¹) (Figs. 6d-f). It extended ~3 km into the canyon interior. Fluorescence values were generally high (0.5-1.1 μg·L⁻¹) in the upper 400 m of the water column (Fig. 6e). Below, a relatively cooler, saltier, less oxygenated, and slightly denser (~29.55 kg·m⁻³) water mass was apparent around 350-400 m depth (Figs. 5d-f). Deeper into the canyon (> 400 m depth), a much warmer (T > 13 °C) and saltier (S ~ 38.4) water mass with lower SPM concentrations and fluorescence values was observed (Figs. 5d-f and 6d-f).

Further offshoredowncanyon, the T2 transect crossed the middle sections of the Cap de Creus Canyon and covered the entire water column down to 850 m deptha depth of 850 m (Figs. 5g-i and 6g-i). The upper 250 m showed a remarkably homogeneous water mass throughout the canyon. It was characterized by temperatures of 13.2-13.4 °C, salinities of ~38.2, relatively high dissolved oxygen values (197 μmol·kg⁻¹), and low SPM concentrations (0.3 mg·L⁻¹) (Figs. 5g-i and 6g-i). Below this layer, and down to 380 m depth, a much colder (12.2-12.3 °C), fresher (38.1), highly oxygenated (200-203 μmol·kg⁻¹) and moderately turbid (0.8-1.0 mg·L⁻¹) water mass was observed (Figs. 5g-i and 6g-i). This water mass only occupied the southern flank of the canyon and extended approximately 2.5 km into the interior of the canyon (Figs. 5g-i and 6g-i). Fluorescence values ranged from 0.18 to 0.60 μg·L⁻¹ throughout the canyon from the surface to ~380 m depth above the 29.0 kg·m⁻³ isopycnal (Fig. 6h). Finally, between 400 m and 850 m depth, the water column was characterized by temperatures of ~13.1 °C, salinities of 38.4, and relatively lower oxygen concentrations, fluorescence values, and SPM concentration (Figs. 6g-i).

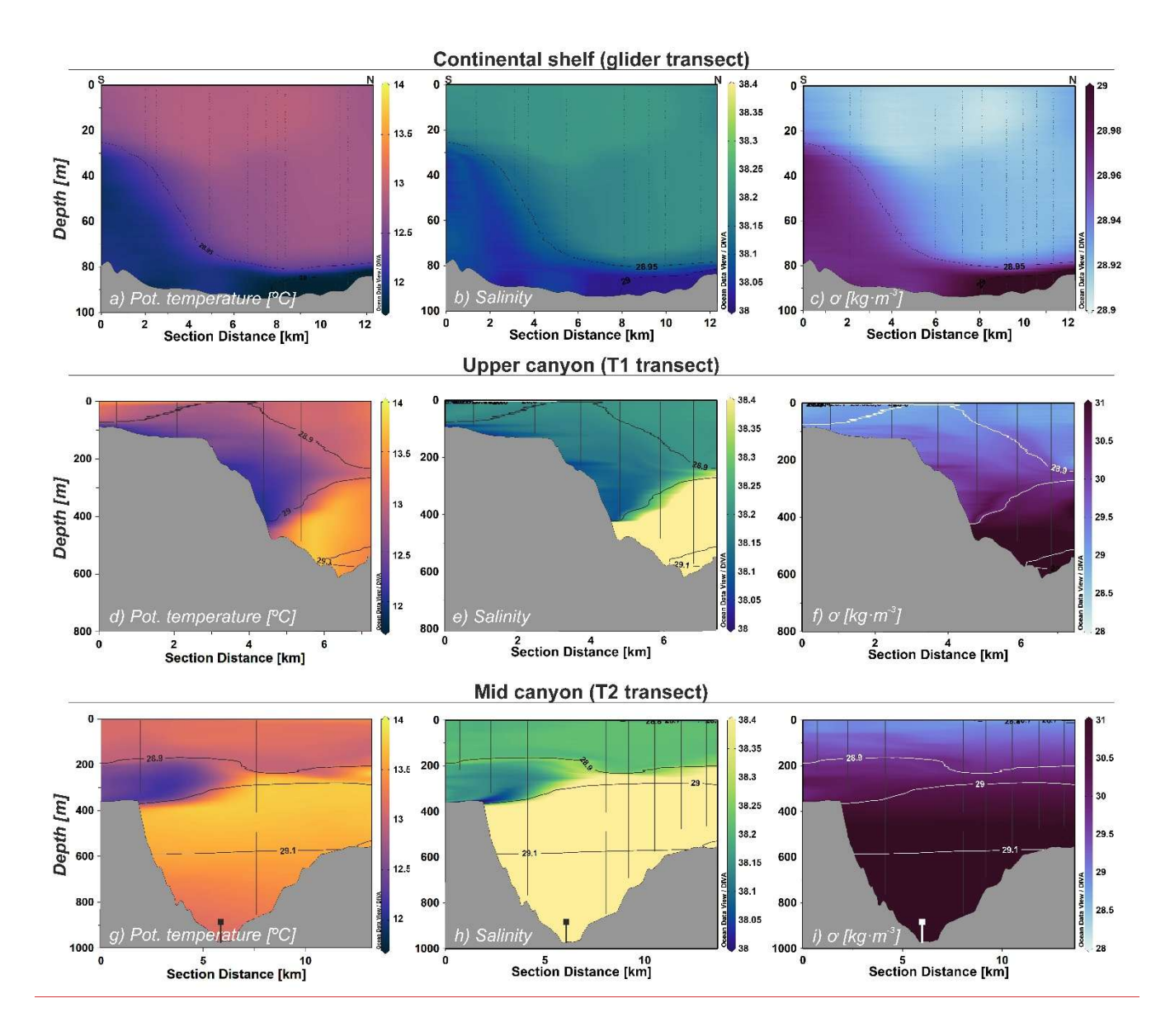


Figure 5. Contour plots of potential temperature (°C), salinity, and potential density (σ, kg·m⁻³) at (a-c) the continental shelf (glider transect) and the Cap de Creus Canyon during (d-f) T1 transect and (g-i) T2 transect (FARDWO-CCC1 cruise). Note that for panels (a-c), the section distance goes from south to north, whereas for panels (d-i), the section distance represents a southwest-northeast direction, crossing the southern flank of the canyon. Note the change in the density scale in panel (c).

97

\$00

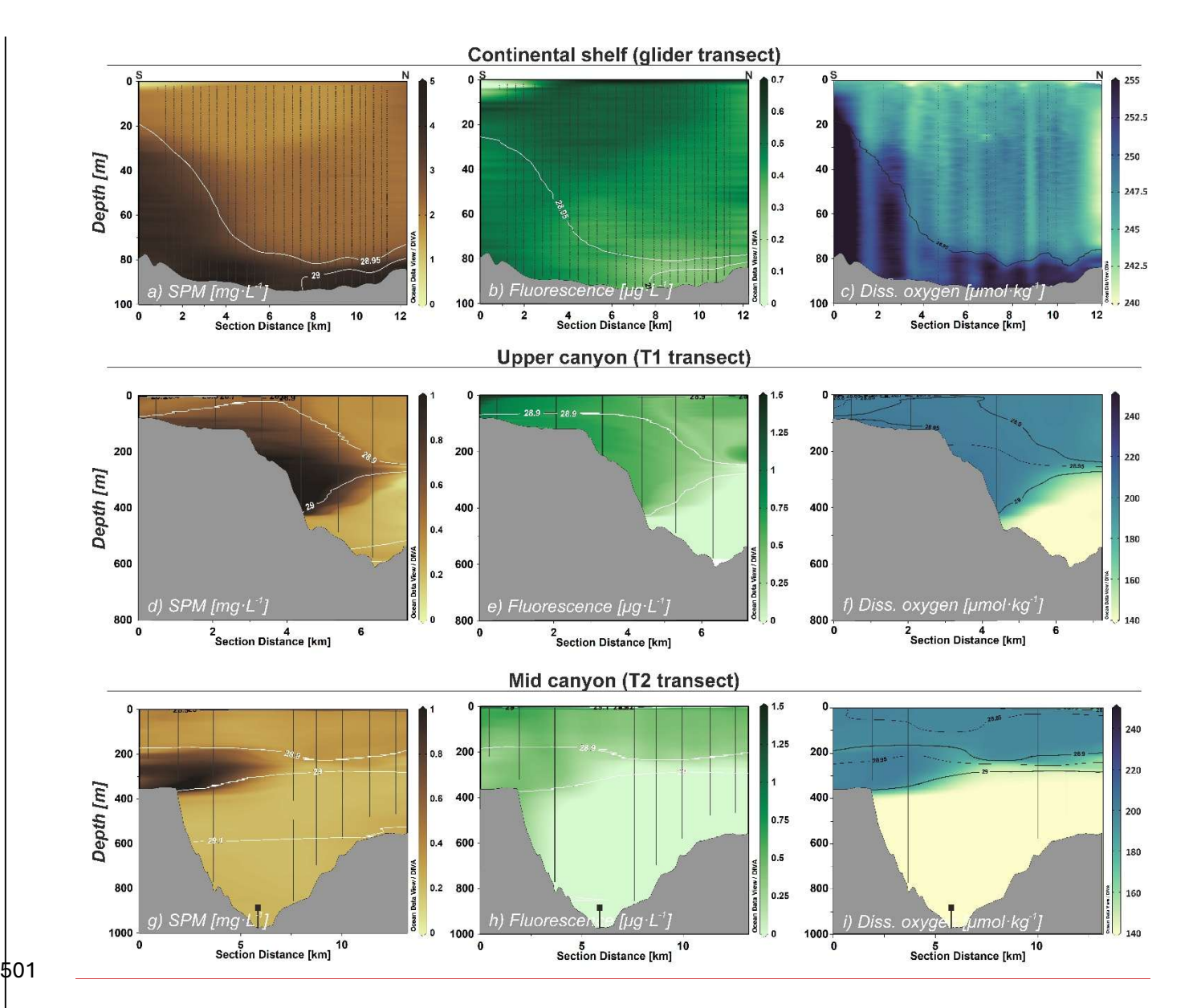


Figure 6. Contour plots of SPM concentration (mg·L⁻¹), fluorescence (μg·L⁻¹), and dissolved oxygen concentration (μmol·kg⁻¹) at (a-c) the continental shelf (glider transect) and at the Cap de Creus Canyon during (d-f) T1 transect and (g-i) T2 transect (FARDWO-CCC1 cruise). Note that for panels (a-c), the section distance goes from south to north, whereas for panels (d-i) the section distance represents a southwest-northeast direction, crossing the southern flank of the canyon. Note the change in the dissolved oxygen scale in panel (c).

4.3.2. Currents

502

\$03

\$04

\$05

506

507

508

509

510

\$11

512

513

\$14

\$15

\$16

\$17

At the continental shelf, current velocity measurements indicated a fairly homogeneous current field (Figs. 7a-c). Cross-shelf currents exhibited low velocities (< 0.1 m·s⁻¹), predominantly eastward (Fig. 7a), while along-shelf currents were slightly higher (0.1-0.15 m·s⁻¹) and predominantly southward (Fig. 7b). The spatial distribution of currents averaged within the dense water vein-plume (defined between the 28.9 and 29.0 kg·m⁻³ isopycnals) shows that dense shelf waters flowed south/south-eastward along the continental shelf adjacent to the Cap de Creus Canyon, with speeds generally around 0.15 m·s⁻¹ (Fig. 7c). However, in the southern part of the section, currents were stronger, exceeding 0.2 m·s⁻¹ (Fig. 7c).

In the Cap de Creus Canyon, at the <u>upper section (T1 transect)</u>, current velocity measurements revealed the highest speeds from the surface to 400 m depth at the southern canyon flank (Figs. 7d, e). <u>The zonal current velocity (E-W) Across-canyon currents</u> reached up to 0.3 m·s⁻¹ <u>eastwardeastward</u> (Fig. 7d), while <u>the meridional current velocity (N-S) alongwas</u> <u>eanyon currents were</u> primarily <u>downcanyonsouthward</u>, with velocities between 0.1 and 0.2 m·s⁻¹ (Fig. 7e). These currents

\$24

\$25

\$26

\$27

\$28

\$29

\$30

appeared relatively confined within the canyon axis, with a pronounced down-canyon component (Fig. 7f). Further offshore, At the mid-canyon section (at the T2 transect), the highest current velocities were observed between 200 and 400 m depth (Figs. 7g, h). Across-canyon The zonal current velocities were more pronounced, and reached values of ~0.15 m·s⁻¹ eastward (Fig. 7g), while the meridional — Along-canyon—current velocities were slightly smaller, ranging from 0.1 to 0.12 m·s⁻¹ southward (Fig. 7h). At On the southern flank, currents were generally weaker (~0.1 m·s⁻¹) and predominantly southward, whereas at the northern canyon flank, these were stronger (~0.2 m·s⁻¹) and mainly oriented towards the southeast (Fig. 7i).

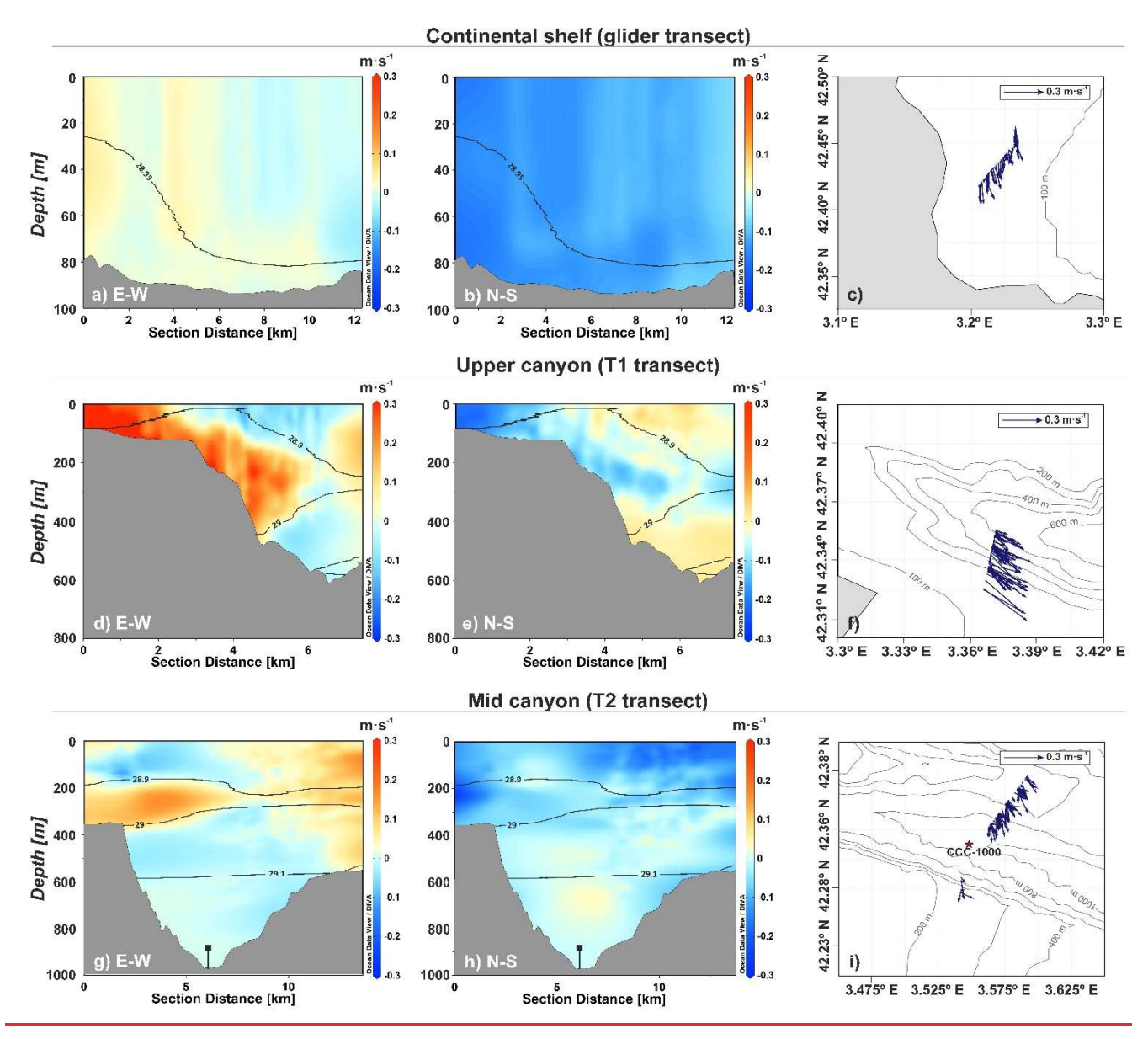


Figure 7. Contour plots of currents measured at (a-b) the continental shelf (glider transect) during the glider survey and at the Cap de Creus Canyon during (d-e) T1 transect and (g-h) T2 transect (FARDWO-CCC1 cruise). In panels (a-b), eEastward and northward current velocities are positive, while westward and southward current velocities are negative. Panels (d and g) represent across canyon current velocities, while panels (e and h) represent along canyon current velocities. Panels (c, f, and i) display stick plots representing the depth-averaged currents within the dense water vein associated with dense waters for the three transects, defined between the 28.9 and 29.05 kg·m⁻³ isopycnals.

5. Discussion

531

532

\$33

\$34

\$35

\$36

\$37

\$38

\$39

\$40

\$41

\$42

\$43

544

\$45

\$46

. 547

\$48

\$49

\$50

\$51

\$52

553

554

555

5.1. Forcing conditions during winter 2021-2022

The winter The fall-winter period of 2021-2022 was characterized by two distinct periods: a first typical winter phase from December to January with several short northerly and northwesterly windstorms that caused stratified water column with short northerly storms that caused continuous heat losses in the GoL followed by a second period from February to March dominated by marine storms and lower heat losses (Fig. 3a). and moderate river flooding (Fig. 3). During the first this period, the averaged sea-atmosphere heat loss was around -158 W·m⁻² (Fig. 3a). In contrast, the second period showed reduced mean heat losses (-70 W·m⁻²) (Fig. 3a). Overall, averaged sea-atmosphere heat loss for the whole winter was -150 W·m⁻² (Fig. 3a), slightly lower than typical mild winters in the GoL (-200 W·m⁻²) and much lower than severe winters such as 2004-2005 (-300 W·m⁻²) (Schroeder et al., 2010). Despite this, seven days of easterlies/southeasterlies were recorded, similar to the winters of 2010 2011 and 2016 2017, which had 10 days (Mikolajezak et al., 2020). In contrast, the cold, dry winter of 2011 2012, a notable year for dense water formation, had only one day of easterly winds (Durrieu de Madron et al., 2013).

Averaged sea-atmosphere heat loss from October 2021 to early March 2022 was of -150 W·m⁻² (Fig. 3a), lower than typical mild winters (200 W·m⁻²) and much lower than severe winters such as 2004-2005 (-300 W·m⁻²) in the region (Schroeder et al., 2010). Hintense short episodes of heat loss eat loss peaked at (-500 W·m⁻²-) occurred in November 2021 and January 2022 (Fig. 3a), which likely contributed to . This may have caused significant surface water cooling and buoyancy loss, especially on the inner shelf (Figs. 3e-g). Water temperature dropped below 12.9 °C in late December/early January (Figs. 3e) and 8a) and below 12 °C in mid/late February (Figs. 3e) and 8b), while shelf water density increased to . Shelf water density increased to -28.9-28.95 kg·m⁻³, exceeding the pre-winter maximum of 27.9 kg·m⁻³ (Fig. 8a)3g). This allowed shelf waters formed over the GoL's shelf to spread as a near-bottom layer across the mid and outer shelf and cascade downslope ese conditions led to destratification of the water column and allowed shelf water to plunge down the slope and spread as a bottom layer across the mid and outer shelf (Figs. 3 and 8a8b, cb). This probably likely marked the beginning of the easeade DSWC period, a scenario consistent with previous studies in the GoL (Dufau-Julliand et al., 2004; Durrieu de Madron et al., 2005; Canals et al., 2006; Ulses et al., 2008a).

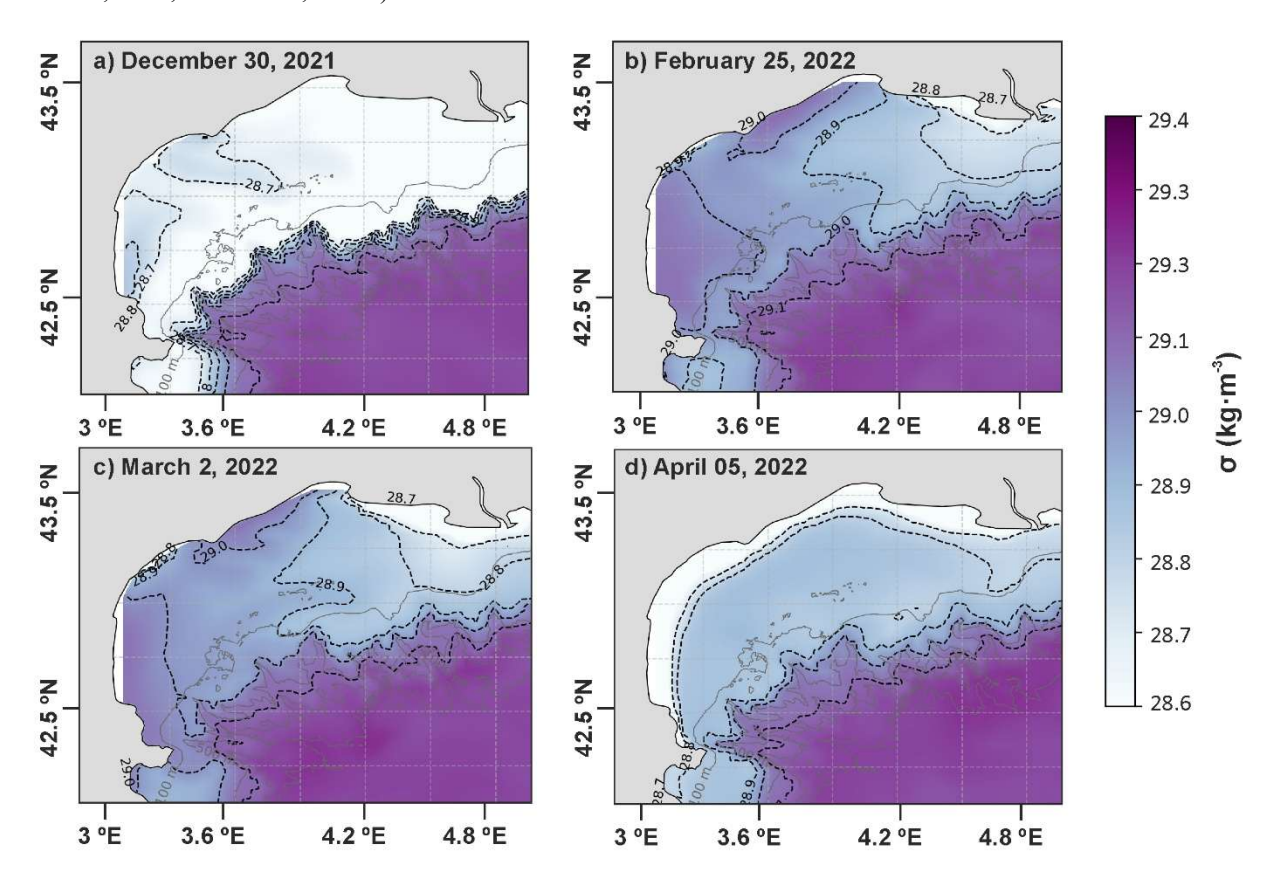


Figure 8. Bathymetric maps of the Gulf of Lion (GoL) showing the potential density anomaly temperature at bottom for four days during the winter of 2021-2022: (a) December 30, 2021; (b) February 25, 2022; (c) March 2, 2022; and (d) April 5, 2022. Density contours (black) are displayed every 0.1 kg·m⁻³. Data has been obtained from the Mediterranean Sea Physics Reanalysis product (Escudier et al., 2020; 2021).

Moreover, during winter, especially throughout February and March 2022, the region was impacted by several easterly/southeasterly windstorms, often associated with increased freshwater discharge from the Rhône River and the coastal rivers (Fig. 3d). Such freshwater inputs are commonly observed during mild winters in the region and can locally reduce salinity and density over the shelf (Ulses et al., 2008a; Martín et al., 2013; Mikolajczak et al., 2020). In contrast, winters favorable to IDSWC, such as 2004-2005, 2005-2006, and 2011-2012, are marked by stronger heat losses, sustained cooling and notably low river discharge (Ulses et al., 2008b). For example, during winter 2004-2005, the Rhône River discharge averaged only ~1400 m³·s⁻¹ between December and March, which is below the mean annual discharge (1920-2007) of 1850 m³·s⁻¹ (Pont et al., 2002; Provansal et al., 2014). These conditions allowed shelf waters to gain potential densities exceeding 29.1 kg·m⁻³, which are sufficient to break through the Eastern Intermediate Water (EIW) layer and generate deep cascading, even reaching depths > 2000 m (Font et al., 2007; Durrieu de Madron, 2013; Palanques and Puig, 2018). Contrary, during the mild winter of 2021-2022, although winter cooling led to shelf water densification (~28.95 kg·m⁻³), dense waters were not dense enough to overcome the EIW and reach the deep basin. Instead, they spread along the mid-shelf and upper slope (Fig. 8b, c). The cyclonic circulation on the western part of the shelf, driven by the prevailing northerly and north-westerly winds (Ulses et al., 2008a; Bourrin et al., 2008Estournel et al., 2003), may have facilitated the promoted the transport of these dense shelf waters along the coast (Fig. 7b). The narrowing of the shelf near the Cap de Creus Peninsula further accelerated the overflow of dense shelf waters into the upper slope, mainly cascading into the westernmost canyons (i.e., Lacaze-Duthiers and Cap de Creus Canyons) (deeper sections of the margin (Ulses et al., 2008a). However, the fresh water supplied by the rivers discharging into the GoL likely prevented a significant increase in shelf water density. During that winter, several flood events impacted the Rhône River and the smaller coastal rivers discharging into the GoL (Fig. 3d). In late December, the Rhône River discharge reached an exceptional daily value of over 5,000 m³·s⁻¹ (Fig. 3d), which represents approximately three times the mean annual discharge of this river. Other moderate increases of the Rhône River discharge (> 2,000 m³·s¹) were recorded earlier during autumn as well as in early winter (Fig. 3d). As a result of these inputs, the salinity and density of shelf waters slightly decreased, particularly during early January (Figs. 3e, f).

Nevertheless, the

\$56

557

\$58 559

560

\$61

\$62

\$63

\$64

\$65

\$66

\$67

\$68

\$69

\$70

\$71

\$72

\$73

\$74

. 575

\$76

\$77

\$78

\$79

\$80

\$81

\$82

\$83

584

\$85

\$86

\$87

\$88

589 590

\$91

\$92

\$93

\$94

595

\$96

\$97

\$98

The freshwater inputs during this period, combined with the mild atmospheric meteorological conditions during winter 2021-2022 prevented the transport of dense waters into the deeper sections of these canyons. In fact, the mooring data acquired in the Lacaze-Duthiers and Cap de Creus canyons clearly indicate that dense shelf waters did not reach the deeper canyon sections during that winter. In both moorings, the recorded current speeds remained below 0.2 m·s⁻¹, temperatures were nearly constant (13.5 °C), and SPM concentrations were < 1 mg·L⁻¹ (Fig. 4), indicating the absence of a deep cascading. For IDSWC events, previous mooring data have registered much colder near-bottom temperatures (11-12.7 °C), stronger down-canyon velocities (> 0.8 m·s⁻¹), and significantly higher SPM concentrations (~40 mg·L⁻¹) (Canals et al., 2006), prevented a significant increase in the density of shelf waters (Herrman et al., 2008; Mikolajczak et al., 2020). This limitation, in turn, restricted the intrusion of dense shelf waters into deeper sections of the slope and the westernmost canyons, including the Lacaze Duthiers and the Cap de Creus Canyons (Fig. 4g).

5.2. Dense shelf water cascading in Advection of dense shelf waters into the Cap de Creus Canyon

During the winter 2021-2022, the density anomaly of shelf waters around 28.95 kg·m⁻³ was not high enough to cause cascading beyond 500 m depth (Fig. 8c). Instead, the newly formed dense shelf waters preferentially flowed southward along

the coast, and only a portion was drained by the westernmost eanyons (Fig. 8c). Dense shelf waters preferentially flowed into the upper and intermediate water column and did not cascade into the deeper reaches of Lacaze Duthiers and Cap de Creus eanyons. This was evidenced by the low current speeds (< 0.2 m·s⁻¹), nearly constant temperatures (~13.5 °C), and low SPM concentrations (< 1 mg·L⁻¹) recorded at LDC-500, LDC-1000, and CCC-1000 mooring sites (Fig. 4). These characteristics are comparable to those reported during the mild winters of 2003–2004 (Ulses et al., 2008a) and 2010–2011 (Martín et al., 2013). In both winters, the density anomaly of shelf waters (28.8–28.9 kg·m⁻³) similarly limited the cascading to depths greater than 350–400 m. In contrast, during the extreme winters of 2004–2005, 2005–2006, and 2011–2012, density anomalies exceeding 29.2 kg·m⁻³ allowed the cascading of dense shelf waters to depths > 2,000 m, reaching the bottom of the basin (Canals et al., 2006; Font et al., 2007; Palanques et al., 2009, 2012; Durrieu de Madron et al., 2013).

99

In early March 2022, during the glider survey, the signature-presence of dense shelf waters (T < 13-12.9 °C and S < 38.4) was detected at the narrow continental shelf adjacent to the head of the Cap de Creus Canyon during the glider survey (Figs. 5a-c). Previous works have demonstrated that, once after dense shelf waters reach the Cap de Creus Peninsula, they are water formation in the GoL, much of this water is pushed southward along the shelf by Tramontane winds and the general circulation (Ulses et al., 2008a; Bourrin et al., 2008). Once it encounters the Cap de Creus Peninsula, the dense water flow is deflected and start and dense shelf waters begin to pool the outer shelf until they spill into the Cap de Creus Canyon from the southern flank (Dufau-Julliand et al., 2004; Canals et al., 2006; DeGeest et al., 2008).

This was first suggested when a large field of sedimentary furrows was found oblique to the canyon axis (Canals et al., 2006; Lastras et al., 2007), and then demonstrated through modelling by Dufau Julliand et al. (2004) and by further observations by DeGeest et al. (2008), which found that the southern rim of the canyon is an area of sediment bypassing due to episodic strong currents during cascading events. The relatively steep bathymetry of the inner shelf, in combined combination with the prevailing south-eastward currents at the inner shelf (Figs. 7a-c), facilitated the transport of dense waters to the into the upper section of the Cap de Creus Canyon. Most likely, these dense waters were pushed into the canyon by cascading currents or storm-induced downwelling processes associated with northerly/north-westerly winds (Fig. 3b), as , as it was observed during previously documented for the mild the winter of 2010-2011 (Martín et al., 2013). Within the upper canyon section, the FADWO-CCCI-T1 transect showed a vein of cold, fresher water, and rich in oxygen and chlorophyll-a between 100 and 350 400 m depth (core depth: 380 m) (Figs. 5d-f and 6d-f), above the EIW f(~400 ound at ~500 m depth) (Fig. A1). This flow traced the export of a vein of coastal dense waters exported from the shelf towards the upper continental slope, which contributed to the body of WIW (Figs. 5d-f and A1).

The WIW likely formed on the outer shelf of the GoL during winter through intense surface cooling and convective mixing of the AW, and theneould have been formed earlier by DSWC events affecting the upper slope of the GoL (Lapoyade and Durrieu de Madron, 2001; Dufau Julliand et al., 2004; Durrieu de Madron et al., 2005; Juza et al., 2019), which are especially intense between late January to early March, and then advected southward to the Cap de Creus Canyon by the general circulation (Lapouyade and Durrieu de Madron, 2001; Dufau-Julliand et al., 2004; Juza et al., 2019).

If we examine the hydrodynamics of the dense water plume, it exhibits characteristics consistent with the "head-up" configuration described in Shapiro and Hill (2003), in which most of the dense water remains upslope while only a thin tail extends downslope. This configuration suggests a limited downslope export of dense waters. To further characterize the flow regime of the plume, we estimated two dimensionless numbers: the Richardson number (Ri) and the Froude number (Fr), both of which provide insights into the stability and dynamical behaviour of stratified flows.

The Ri is a ratio between the Brünt-Väisäla frequency squared (N²) and the vertical shear of the horizontal velocity (S²), and describes the tendency of a stratified flow to remain laminar or become turbulent (Monin and Yaglom, 1971). For this calculation, we used temperature, salinity, and E-W current velocities from CTD and LADCP measurements acquired during the cruise. Ri values showed a general increase between 150 and 300 m depth, which roughly corresponds to the vertical extent of the dense shelf water plume (Fig. C1). The maximum Ri observed reached 0.18 at 270 m depth in the upper canyon,

and 0.16 at 180 m in the mid canyon. These values are below the critical threshold of 1 that separates laminar (Ri >1) from turbulent flow regimes, thus indicating a predominantly turbulent flow (Mack and Schoeberlein, 2004). This suggests that fluid instabilities likely enhanced vertical mixing and lateral spreading of the dense water plume.

50

51

53

54

55

56

57

58

59

61

67

73

75

76

77

78

79

81

83

84

Complementary, we estimated the Froude number $(Fr = U/\sqrt{g'h})$, following the approach by Cenedese et al. (2004), which distinguishes between laminar, wavy, and eddying flow regimes in dense bottom currents over slopes. Using a representative current velocity (U) of $0.18 \text{ m} \cdot \text{s}^{-1}$, a dense layer thickness (h) of 100 m, and a reduced gravity (g') of $2.67 \cdot 10^{-4} \text{ m} \cdot \text{s}^{-2}$, we obtained Fr ~1.10. This value lies just above the critical threshold of 1, indicating a supercritical flow regime where inertial forces become more significant, potentially favoring more unsteady and turbulent flow conditions (Cenedese et al., 2004).

Within the Cap de Creus Canyon, coastal the dense shelf waters vein flowed predominantly along the southern canyon flank, associated with accompanied by increased SPM concentrations (Figs. 6 and 7). This suggests that during this MDSWC event, dense waters the downwelling of dense coastal waters transported resuspended sediment particles into the canyon down to intermediate depths (Fig. 6d). The time series of river water discharge from the Rhône River and the smaller coastal rivers data does not seem to indicate a important freshwaters and sediment inputs prior to the cruise significant influence of the transport of sediments to the canyon (Fig. 3d). In fact, both the Rhône River and the smaller coastal rivers had low-relatively low discharges before and during the FARDWO-CCC1 Ccruise (Fig. 3d). This points to storm-waves and cascading-induced currents, rather erosion generated by storm waves or strong currents by cascading rather than riverine input discharge, as the main mechanisms source of sediment resuspension and transport. This is consistent with previous findings by Estournel et al. (2023), who described that, during the mild winter of 2010-2011, storm-induced downwelling events contributed to the remobilization of shelf sediments that fed the upper section of the Cap de Creus Canyon and along the North Catalan shelf. In fact, during mild winters, most of the sediment particles associated with the dense water vein flowing along the southern flank of the canyon. Actually, most of the sediment delivered by the GoL's rivers remains relatively close to their mouths after floods and it is later remobilized by storm waves under highly energetic conditions (Guillén et al., 2006; Estournel et al., 2023). In addition, the Additionally, increased fluorescence values observed within the dense water vein plume (Fig. 6e) suggests the mixing of terrestrial sediments with phytoplankton cells (Figs. 6e, h). Phytoplankton blooms, which typically peak between December and January, likely contributed newly produced biological particles to GoL's shelf waters, the dense water vein, thereby enhancing the transport of organic matter into the canyon during the observed MDSWC event (Fig. B1; Fabres et al., 2008).

The dense water vein-plume continued flowing down-canyon to the mid-canyon section, where it contributed to the WIW body that extended to depths of 380 m (Figs. 5g-i). At these depths, enhanced SPM concentrations were observed on the southern flank, contrasting with the clear waters on the northern canyon flank (Fig. 6g). The contrast in SPM concentrations between the flanks of the Cap de Creus Canyon actually reflects its marked asymmetric morphology and hydrodynamics. One key aspect is the very narrow adjacent shelf (2.5 km), which brings the southern rim of the canyon into close proximity with the coast (Lastras et al., 2007; Durán et al., 2014). The canyon itself presents very dissymmetric walls: the northern canyon wall is relatively smooth, with fine-grained silty clays and relatively high accumulation rates (up to 4.1 mm·yr⁻¹), indicative of a depositional area. On the other hand, the southern flank has erosional features (exposed bedrocks and gullies), and coarser sediments such as gravel. These characteristics, along with lower accumulation rates (~0.5 mm·yr⁻¹), suggest active sediment transport and bypassing processes (Lastras et al., 2007; DeGeest et al., 2008). In addition, other studies have evidenced the presence of furrows oblique to the canyon axis, which have been interpreted as signatures of DSWC events over the southern canyon wall (Canals et al., 2006). This has been later confirmed through modeling and observations (DeGeest et al., 2008), which also identified episodic strong currents in the southern canyon rim during cascading events in this area. Furthermore, the conceptual model proposed by DeGeest et al. (2008) suggest that the coastal current forms an eddy over southwestern shelf near the Cap de Creus headland (Davies et al., 1995), which likely steers dense water flows and sediment preferentially toward

the southern canyon rim (DeGeest et al., 2008). Altogether, these morphological and hydrodynamic features offer a plausible explanation for the enhanced SPM concentrations observed along the southern canyon wall in both upper- and mid-canyon sections during our study (Figs. 6d, g).

85

87

Our data also show that dense waters along the southern canyon flank shifted from a predominantly southeastward direction in the upper-canyon section to a more southward direction in the mid-canyon section (Figs. 7f, i). This transition suggests that, as This asymmetry has also been observed in sediment accumulation rates within the canyon, with higher rates on the northern flank and lower rates or erosion on the southern flank (DeGeest et al., 2008). These findings suggest that the southern flank acts as a bypass area during DSWC events. Southeast-flowing currents transport sediment particles along this flank, contributing to the formation of bottom and intermediate nepheloid layers (Figs. 6d, g; DeGeest et al., 2008). Meanwhile, the dense water flow within the canyon shifted from a down-canyon direction in the upper canyon section to a more southward direction in the mid-canyon section (Figs. 7d i). This indicates that dense waters reached their equilibrium depth. As the canyon topography opens, dense waters they are no longer confined by its walls and the eanyon and began begin to veer towards southward, the south, following the continental slope (Millot, 1990). Previous studies have shown that part of these waters have shown that part of these dense waters can continue flowing southward, skirting the Cap de Creus Peninsula and crossing the Gulf of Roses and before reaching the neighbouring Palamós and Blanes Canyons (Zúñiga et al., 2009; Ribó et al., 2011). This is supported by the presence of a shallow NNE-SSW oriented channel that extends from the narrow shelf of the Cap de Creus Canyon to the head of the Palamós Canyon (Durán et al., 2014). During MDSWC events, this channel facilitates the along-slope transport of dense waters (particularly WIW) and associated suspended sediment towards the Palamós Canyon (Ribó et al., 2011; Martín et al., 2013). A similar mechanism may have occurred during the studied winter here (2021-2022), when WIW could have been advected southward through this channel and eventually reached neighbouring canyons Similarly, the WIW observed during the present study could have also reached the Palamós Canyon during the winter of 2021 2022, following the along margin circulation, as previously documented in this submarine canyon during the the mild winter of 2017 (February March) (Arjona-Camas et al., 2021).

5.3<u>. Spatial and temporal variabiliaty</u> Dense shelf water export of dense shelf water export in the Cap de Creus Canyon

At the 5.3.1 Spatial variability of the export: observational data

The total transport associated with the dense water vein in the Cap de Creus Canyon and its adjacent shelf was estimated for each CTD profile conducted during both the FARDWO CCC1 Cruise and the glider survey in early March 2022. This estimation was based on simultaneous SPM concentration and current speed measurements. For the glider survey, SPM data were obtained from the WetLabs FLBB sensor, and current speed from the AD2CP. For the CTD transects, SPM concentrations were obtained from the SeaPoint sensor on the CTD probe, and current speed was recorded using the LADCP. Transport was integrated for each profile and across the section to estimate the total export associated with dense shelf waters. SPM transport was calculated by multiplying the estimated water transport by the SPM concentrations associated with the dense water vein. For the CTD transects, transport was calculated in vertical cells of 8 m (the bin size of the LADCP) and integrated over the different profiles across the sections. SPM concentration data were resampled to match the vertical resolution of the current speed measurements. Finally, the SPM transport was calculated using the same approach as in the glider section.

Dense shelf water transport across the continental shelf transect (Fig. 1), dense water transport was estimated at 0.7 Sv and 10⁵ metric tons of SPM. from glider data. In the upper canyon section (T1 transect), the total transport associated with the dense waters flow was 0.3 Sv, including 10⁵ tons of suspended particulate matterSPM. These values are comparable to those observed during the mild winter of 2010-2011 in the Cap de Creus Canyon, for which Martín et al. (2013) estimated a

28

29

30

731

732

733

734

735

736

737

738

739

740

741

742

743

44

745

746

47

748 749

750

751

752 753

754

755

756

757

'58

759

760

761

762

763

total transport of 105 metric tons of SPM though the southern canyon wall. Further downslope-, at At-the mid-canyon section (T2 transect), transport across the southern flank decreased to 0.05 Sv, with roughly 10⁴ metric tons of SPM. This transport reduction between the upper and mid-canyon sections suggests that most of the dense water either remained on the shelf, skirted around the Cap de Creus headland, or cascaded only into the upper canyon. Part of the dense shelf waters could have also followed the shallow channel located between 100 and 150 m depth, as previously discussed (see Fig. 4 in Durán et al., 2014) suspended particulate matter. These values are comparable to those observed during the mild winter of 2010-2011 in the Cap de Creus Canyon (Martin et al., 2013). The transport decrease between T1 and T2 suggests that most dense water flow remained on the shelf and shelf edge around the Cap de Creus Canyon Peninsula, rather than fully cascading into the canyon. This indicates that during mild winters, the Cap de Creus Canyon acts only as a partial sink for cascading waters.

Since our observations provided only a snapshot of this MDSWC event, we used

5.3.2 Temporal variability of the export: reanalysis data

The MedSea-reanalysis data to determine its temporal extent and to place it in the broader context of cascading events in the Cap de Creus Canyon over the past two decades. We assessed the reliability of the MedSea by comparing it with our CTD observations. In particular, we compared depth-averaged temperatures within the dense water plume (150-390 m depth) at stations where dense waters (T< 12.9 °C) were detected, using the root mean square error (RMSE) statistical method. The RMSE errors were consistently low across all stations (< 0.2 °C) (Table 1), indicating a good agreement between both datasets. These results, along with the detailed validation presented in Fos et al. (2025), support the use of the MedSea reanalysis product for studying DSWC in this region. In that study, the authors compared the MedSea output with long-term mooring data from the Cap de Creus and Lacaze-Duthiers canyons, and showed that, at 1000 m depth, the MedSea reproduces 84% of individual DSWC events within the same week and 56% on the exact date (Fos et al., 2025).

Table 1. Comparison of depth-averaged temperatures within the dense water plume derived from observations and reanalysis, with corresponding root mean squared errors (RMSE).

<u>Stations</u>	Observed temperature (°C)	<u>Reanalysis</u> <u>temperature (°C)</u>	RMSE (°C)
<u>T1-01</u>	<u>12.41</u>	<u>12.42</u>	<u>0.17</u>
<u>T1-02</u>	<u>12.55</u>	<u>12.46</u>	<u>0.18</u>
<u>T1-03</u>	<u>12.34</u>	<u>12.42</u>	<u>0.19</u>
<u>T1-04</u>	<u>12.76</u>	<u>12.42</u>	<u>0.21</u>
<u>T2-01</u>	<u>12.96</u>	<u>12.71</u>	<u>0.15</u>
<u>T2-02</u>	<u>12.68</u>	<u>12.65</u>	<u>0.04</u>
<u>T2-03</u>	12.72	12.67	0.05

Daily reanalysis data indicated that the export of dense water was consistently higher in the upper-canyon section than in the mid-canyon section throughout winter 2021-2022 (Fig. 9a), consistent with observational results. A significant increase of dense water export occurred in late January (0.2 Sv), coinciding with a drop in temperature (T < 12.9 °C) and a slight decrease in potential density to 28.85 kg·m⁻³ (Fig. 9). Although an increase in transport was also detected in the midcanyon section (Fig. 9a), it was notably smaller in magnitude (~0.12 Sv), and the potential temperature time series do not seem to indicate the presence of dense shelf waters in the canyon at that depth (Fig. 9b). Three shallow cascading pulses were further identified in mid- and late February and early March, which had comparable down-canyon transport magnitudes (~0.2 Sv) in the upper canyon section (Fig. 9a). The mid-February pulse was particularly evident in the upper canyon section, which coincided with a temperature drop below 12.5 °C (Fig. 9b) that indicated the arrival of dense waters at this depth. Another shallow cascading was identified in mid-March, representing the strongest transport event in the canyon.

This mid-March event was particularly noted in the upper-canyon section (with ~0.4 Sv) and, to a lesser extent, in the mid-canyon section (~0.1 Sv) (Fig. 9a). The time series of temperature (~12 °C) and the concurrent increases in potential density (~28.87 kg·m⁻³) (Figs. 9b, c) also confirmed the arrival of dense waters at both locations. The enhanced export observed

in mid-March was likely triggered by the easterly/southeasterly storm on March 13 (Figs. 3b, c), which promoted MDSWC into the Cap de Creus Canyon. The role of marine storms as drivers of downwelling and cascading events has been previously documented for other mild winters, such as 2003-2004 and 2010-2011 (Ulses et al., 2008a; Martín et al., 2013). Nonetheless, these transport peaks are lower than the peak transport estimated in the Cap de Creus Canyons during the extreme winter of 2004-2005 for intermediate waters (~0.6 Sv) (Fig. 10), and for deep waters (1.29 Sv) (Fos et al., 2025).

As March progressed, and net heat losses decreased (Fig. 3a), dense water export gradually decreased, eventually ceasing in early April (Fig. 9a). Accordingly, the duration of the cascading period in the Cap de Creus Canyon, defined as the period between the first and last cascading event (Palanques et al., 2006), was approximately two months, from late January to mid-March 2022 (Fig. 9). During this winter, shallow cascading events primarily affected the upper canyon, with a weaker influence further downcanyon in the mid-canyon section (Fig. 9a). Indeed, t

he total volume of dense water exported during the cascading period in winter 2021-2022 was estimated at 260 km³ in the upper canyon section, compared to approximately 11 km³ in the mid-canyon section.

product was used to assess the variability of dense shelf water export in the Cap de Creus Canyon during the mild winter of 2021–2022. This analysis focused on estimating the temporal variability of dense water export along the canyon two cross sections near the T1 and T2 transects (Fig. 9a). Daily reanalysis data on seawater potential temperature and eastward velocities were used to calculate the transport of dense waters at intermediate depths across these sections during autumn, winter, and early spring. The results indicated that export was generally higher in winter, with transport magnitudes being higher in the upper canyon section compared to the mid canyon section (Figs. 9b, c). Similar to our observational data, these results suggest that dense waters did not penetrate deeply into the canyon but remained on the shelf and around the canyon head.

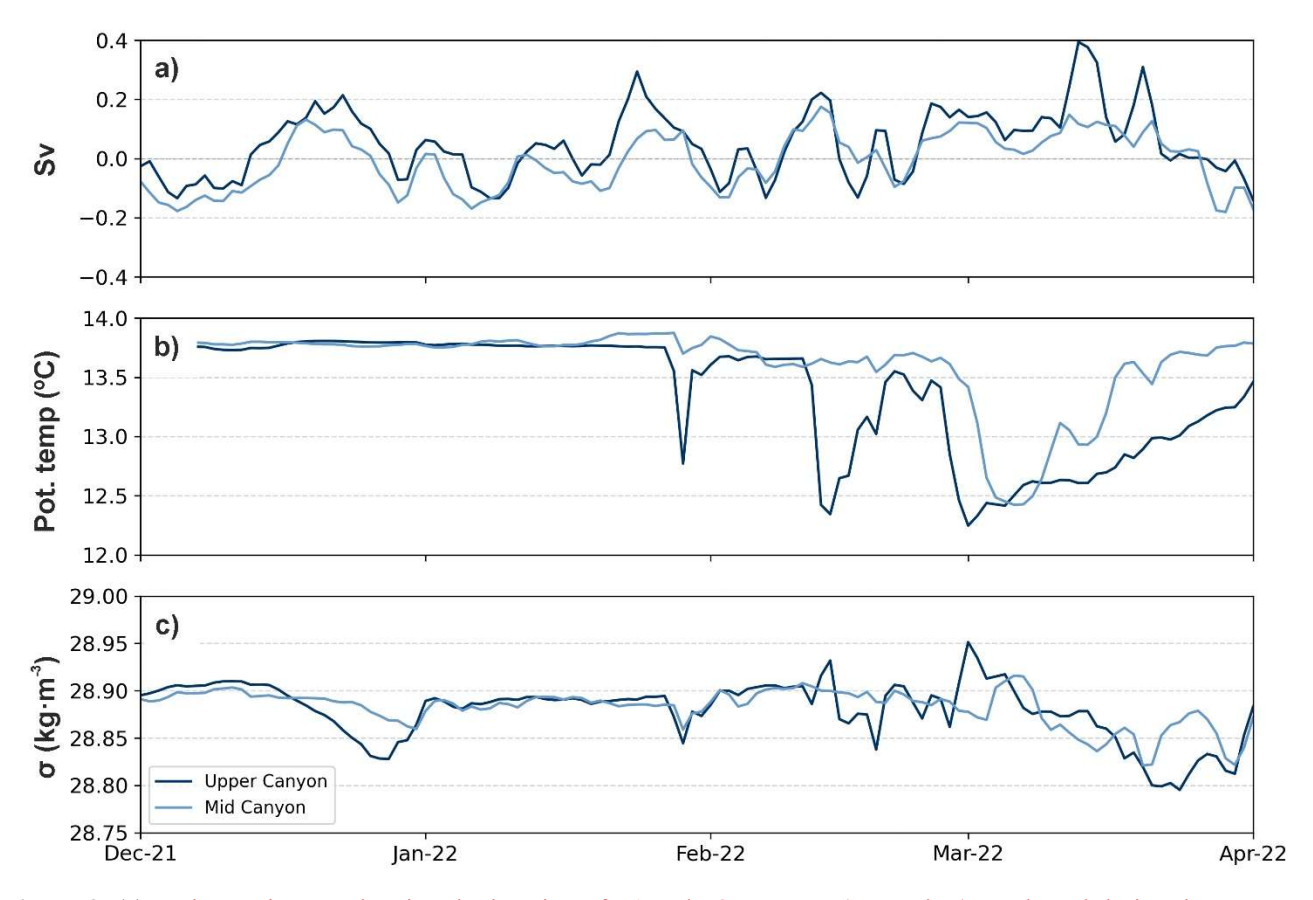


Figure 9. (a) Bathymetric map showing the location of T1 and T2 transects (green dots) conducted during the FARDWO-CCC1 Cruise (March 2022). The two transects used to estimate the temporal variability of the along canyon transport at intermediate depths (350 m depth), located near T1 and T2, are also shown as coloured lines; (b-c) Time series of along-canyon

transport (Sv) of dense waters, (b) potential temperature (°C), and (c) potential density (kg·m⁻³) for (in Sv) and its associated thermohaline characteristics (potential temperature, salinity, and potential density) for two transects: (b) the upper-canyon transect (blue line, near T1dark blue) and (c) the mid-canyon section (orange line light blue), near T2), extracted from the Mediterranean Sea Physics Reanalysis product (Escudier et al., 2020; 2021). In panel (a), pPositive values in the first panels indicate down-canyon transportexport, while negative values indicate up-canyon export.transport.

789

90

791

792

793

794

795

796

797

798

799

\$00

801

802

803

804

\$05

806 807

808 809

\$10

811

\$12

813 814

\$15

\$16

\$17

818

\$19

\$20

\$21

822

823

\$24

825

\$26

\$27

\$28

\$29

\$30

\$31

Moreover, seasonal variability in dense water transport was strongly influenced by meteorological and hydrological conditions (Fig. 3). During autumn, the GoL experienced multiple northerly and northwesterly windstorms (lasting between 1 to 3 consecutive days), along with maximum heat losses that contributed to the cooling and densification of shelf waters (Fig. 3). In early November 2021, the Rhône River discharged 2,492 m³·s¹- of freshwater into the GoL (Fig. 3d). The arrival of this coastal freshwater in the upper canyon section was evident in the reanalysis time series, marked by a slight decrease in salinity and potential density (Fig. 9b).

Winter experienced longer periods of moderate northerly and northwesterly winds (blowing between 5 to 7 consecutive days) and higher discharge from the Rhône River (Fig. 3d). By late December, another significant discharge event from the Rhône River reached the upper canyon section (Fig. 3d), again leading to decreased salinity and potential density (Fig. 9a). The enhanced freshwater input, in addition to wind forcing, likely helped to inhibit the densification of shelf waters over the GoL, preventing their transport into deeper sections of the Cap de Creus Canyon. Notably, no significant temperature increase was observed in the reanalysis time series during this period (Fig. 9b). A significant increase in dense water export occurred in late January, coinciding with the arrival of cold (T < 12.9 °C) and relatively dense waters in the canyon (Fig. 9b). This signal was also detected in the mid canyon section, although with lower transport magnitude (Fig. 9c), suggesting the onset of the cascading period in the canyon. Two additional cascading pulses were also identified in mid February and late-March, both associated with an increase in down canyon transport (Fig. 9b). The increased transport export in March, particularly in the upper canyon section (Fig. 9b), and to a lesser extent in the mid canyon section (Fig. 9c), followed a period of easterly southeasterly winds (Fig. 3b), which most likely triggered or intensified the export within the canyon. The role of marine storms has previously been documented during other mild winters, such as 2003-2004 and 2010-2011, when marine storms played a key role in driving downwelling processes (Ulses et al., 2008a; Rumín-Caparrós et al., 2013).

As spring progressed, neat heat losses gradually decreased (Fig. 3a), likely due to rising atmospheric temperatures. This led to a gradual decline in dense water export, which ceased by early April (Fig. 9a). Accordingly, the duration of the cascading period in the Cap de Creus Canyon, defined as the period between the first and last cascading event (Palanques et al., 2006), was approximately three months, from January to early April 2022 (Figs. 8d and 9).

5.4. Interannual variability of dense shelf water transport and future perspectives of Impact of climate change on DSWC dynamics

Over the past two decades, MDSWC events have been the most common form of dense shelf water export through the Cap de Creus Canyon, as reported in previous studies (Herrmann et al., 2008; Durrieu de Madron et al., 2023), and as further evidenced by the time series of dense water transport estimated from reanalysis data shown in Figure 10. In contrast, IDSWC events have occurred less frequently, typically every 5-7 years, and are often associated with higher transports of dense shelf waters (Fig. 10).

Putting the winter 2021-2022 into perspective, the total dense water transport (260 km³) was approximately half of the total volume simulated for the mild winter of 1998-1999 (500 km³) (Dufau-Julliand et al., 2004), and higher than the total export estimated for the mild winter of 2003-2004 (75 km³) (Ulses et al., 2008a). Compared to the extreme IDSWC event of 2004-2005, one of the most studied events in the GoL, the 2021-2022 MDSWC event accounted for roughly half of the total dense water volume exported through the Cap de Creus Canyon (> 750 km³) (Canals et al., 2006; Ulses et al., 2008b). However, as shown in the reanalysis time series (Fig. 10) and recent numerical simulations (Mikolajczak et al., 2020), mild and extreme

\$32 \$33 \$34 \$35 \$36 \$37 \$38 \$39 \$40 \$41 \$42 \$43

844 845

\$46

847 848

849

\$50

\$51

852

\$53

854

\$55

\$56

857

\$58

\$59

\$60

861

862

\$63

864

865

winters can sometimes reach similar magnitudes of dense water export despite having contrasting atmospheric conditions. For example, during the mild winter of 2010-2011, the total dense water export (1500 km³) was comparable to the extreme winter of 2004-2005 (1640 km³) (Ulses et al., 2008a). The key difference lies in the preferential export pathways: in 2004-2005, 69% of dense shelf water cascaded through the Cap de Creus Canyon down to the deeper parts of the canyon. In contrast, in winter 2010-2011, only 30% of the export occurred through the canyon, while 70% followed along the coast or remained around the upper canyon section (Ulses et al., 2008a; Mikolajczak et al., 2020). This difference may also affect the distribution of suspended sediment, which instead of being advected to deeper canyon areas, is likely redistributed along the shelf or accumulates in the upper canyon. Based on our results, it is very likely that during the winter of 2021-2022, a higher proportion of dense waters and associated suspended sediment was exported along the coast or only generated shallow cascading into the upper canyon, resembling the export pattern observed during the mild winter of 2010-2011. These findings suggest that during mild winters, MDSWC events may primarily influence coastal ecosystems, whereas in extreme winters, IDSWC may significantly impact deep-benthic ecosystems (Mikolajczak et al., 2020).

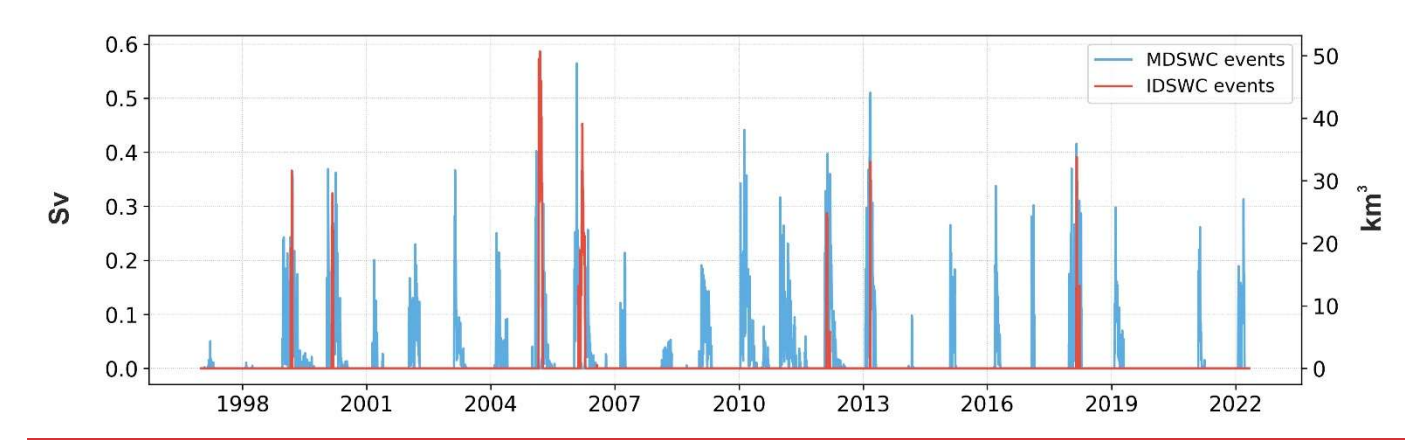


Figure 10. Time series of daily down-canyon transport of dense shelf waters (Sv) from 1997 to 2022, calculated across a central transect in the upper region of the Cap de Creus Canyon (see location in Figure 1). The occurrence and magnitude of IDSWC events is highlighted in red, whereas mild events are highlighted in blue. Data have been extracted from the Mediterranean Sea Physics Reanalysis product (Escudier et al., 2020; 2021).

Our estimates indicate that during the mild winter of 2021–2022, approximately 40 % of the dense shelf water export occurred through the Cap de Creus Canyon, primarily within its upper section, while the remaining 60 % was transported along the coast. This distribution contrasts with the extreme, cold winter of 2004–2005, when nearly 70 % of the export took place through the canyon (Ulses et al., 2008b). These findings suggest that during mild events, DSWC may primarily influence coastal ecosystems, whereas in extreme winters, when dense waters reach deeper areas, DSWC can significantly impact deep-sea habitats (Mikolajezak et al., 2020).

Future climate projections indicate an increasing frequency of mild winters in the northwestern Mediterranean (Herrmann et al., 2008; Durrieu de Madron et al., 2023). Under the IPCC-A2 scenario, DSWC could decline by 90 % at the end of the 21st century (Herrmann et al., 2008). This scenario would drastically reduce both the intensity and depth penetration of DSWC.

Recent studies have already A recent study by Margirier et al. (2020) has already pointed out to a warming and salinification of surface and intermediate waters across the northwestern Mediterranean basin(Margirier et al., 2020), which would increase the stratification of the water column and hinder deep-ocean convection. Such reduction in deep DSWC could strengthen the production of WIW by favouring intermediate-water formation over deep-water ventilation (Parras-Berrocal et al., 2022). Consequently, dense shelf water transport could may become more limited to near-coastal areas or upper-canyon regions, rather than cascading into deeper areas of the continental slope, thus altering the regional hydrology and impacting the Mediterranean Thermohaline Circulation (Somot et al., 2006).

Ongoing sea warming and increasing stratification in the water column could further alter are also expected to impact shelfslope exchanges, reducing IDSWC activity and the associated transport of particulate matter from the GoL to the deep basin (Somot et al., 2006). As a result, the transfer of dense shelf waters and organic matter to the deep sea could would be drastically reduced and mainly redirected along the Catalan shelf or the upper reaches of the Cap de Creus Canyon (Estournel et al., 2023). A decline in the frequency of marine storms could also promote sediment retention in the Rhône River prodelta, reducing the transfer of particulate matter towards the slope and deep basin (Estournel et al., 2023). These changes could significantly alter transport pathways and affect erosion and deposition patterns along the incised submarine canyons of the GoL, and in consequence, have important impacts in deep benthic communities that rely on the arrival of suspended particulate matter. The reduction of deep DSWC would not only reorient the main export routes of dense shelf waters but could also have far reaching consequences for deep-sea ecosystems. Cold water corals, benthic organisms invertebrates, and commercially important species (such as shrimps) may be particularly affected vulnerable, as the limited supply of nutrients and oxygen would hinder their survival (Puig et al., 2001; Pusceddu et al., 2013). In Lacaze-Duthiers Canyon, for instance, Chapron et al. (2020) showed that cold-water coral growth is strongly influenced by the intensity of DSWC events, which modulate their feeding conditions and development. Intense DSWC events cause high budding rates but low colony linear extension by limiting prey capture rates with high current speeds. Mild DSWC events cause high budding rates and high linear extension associated with higher organic matter supply. In contrast, the absence of cascading plumes can cause high mortality (Chapron et al., 2020).

Additionally, the weakening of DSWC could significantly alter sediment transport pathways, affecting erosion and deposition patterns along the incised submarine canyons of the GoL. Changes in sediment dynamics could impact benthic communities that rely on the arrival of suspended particulate matter. For example, Puig et al. (2001) suggested that slope intermediate nepheloid layers, loaded with fine particulate matter rich in organic matter, play a significant role in the settlement of the larvae of benthic species to the seabed, turning nepheloid layers into prime nursery habitats. Regardless of the direction of DSWC's effects on deep-sea ecosystems, it has been demonstrated that even a minor-small loss of biodiversity can result lead to in a major ecosystem collapse (Danovaro et al., 2008), with predictable cascading impacts on ecosystem services, such as including fisheries (Pörtner and Knust, 2007; Smith et al., 2009).

6. Conclusions

\$66

867

\$68

\$69

\$70

871

872

\$73

\$74

\$75

\$76

\$77

\$78

\$79

\$80

\$81

882

883

884

885

\$86

\$87

888

889

\$90

\$91

892

\$93

894

\$95

\$96

\$97

\$98

\$99

900

901

902

903

\$04

905

906

This paper provides a comprehensive observational characterization of shelf-slope exchanges of dense shelf waters and associated SPM in the Cap de Creus Canyon during a MDSWC event. We combined study used a multiplatform approach, combining data from glider datas, ship-based CTD transects, instrumented mooring lines, and reanalysis products data to assess investigate dense water and sediment dense-shelf water and associated sediment transport export in the Cap de Creus Canyon during the mild winter of 2021-2022.

The first part of winter 2021-2022 (December and January) The winter of 2021-2022 was characterized by several days of northerly and north-westerly windstorms, which induced that induced sustained heat loss, surface cooling, and densification of surface waters over the es in the GoL. In contrast, easterly and southeasterly winds during the second part of the winter (February and March) enhanced the export of dense shelf waters to the southwestern end of the gulf, where they cascaded into the upper section of the Cap de Creus Canyon, region, enhancing the formation of dense shelf waters. Nevertheless, the moderate freshwater inputs from the Rhône River and the smaller coastal rivers decreased the density of shelf waters and, consequently, limited their export into deeper sections of Lacaze-Duthiers and Cap de Creus Canyons. In

In-early March 2022, dense shelf waters were observed at the continental shelf during the in the glider transect survey.

These waters cascaded conducted at the continental shelf adjacent to the into the upper canyon down to ~390 m depth, Cap de Creus Canyon. They were transported to the upper canyon section to depths of ~350 m, where they contributed to the formation of the WIW body. Increased SPM concentrations were also observed at the same water depths, likely indicative of a

resuspension process. River discharges were low before and during the FARDWO-CCC1-cruise and, therefore, they were not the main source of suspended sediments-during the downwelling phase. Instead, storm-induced currents associated Erosion induced by the action of storm waves or strong currents by with cascading waters were likely resuspended and transported the main contributor of suspended sediments associated with the dense water vein transported through the canyon. We estimated an export of roughly dense water of ~0.3 Sv and 10⁵ metric tons of sediments on in the upper canyon section. Late winter was marked by persistent northerly and northwesterly windstorms alternated with easterly southeasterly wind events, which reinforced the presence and flushing of dense shelf waters into the Cap de Creus Canyon.

Reanalysis data provided additional temporal context, revealing that the cascading season period lasted approximately two three-months, from late_January to early-mid-March_April_2022. These is-data also showed multiple-several_shallow cascading events_pulses_during this period, with the peak export in late_January and_in_mid-March_associated with an easterly/southeasterly storm that likely pushed dense shelf waters to the canyon. Over the entire cascading period, we estimated a total dense shelf water export of ~260 km³. In terms of volume, the 2021-2022 export was approximately half of that estimated for the mild winter of 1998-1999 and higher than the export simulated for the mild winter of 2003-2004. Compared to the extreme winter of 2004-2005, it represented roughly half of the total dense water volume exported. These contrasts show the episodic and variable nature of DSWC in the GoL. Moreover, it is likely that, during the winter of 2021-2022, a high proportion of dense waters and associated SPM was exported, highlighting the episodic nature of DSWC. This data also showed that much of the dense water export took place along the coast_or generated only shallow cascading into the canyon, resembling the export patterns of previously reported MDSWC events., while only a small portion downwelled into the westernmost canyons incising the GoL (namely Lacaze Duthiers and Cap de Creus canyons) between 200 and 400 m depth.

Future investigations research should benefit from a more detailed exploration of the physical dynamics driving DSWC. More importantly, given the climate change scenario, future studies should focus on the evolution and aim to expand observational datasets, not only within the westernmost canyons incising the gulf but also across the shelf areas. Increasing glider surveys on the GoL's shelf area could improve our understanding of dense water export during weak cascading events under mild winter conditions. Further investigations should also focus on the changes in on the WIW. These studies would help to understand the alterations in the water column properties and changes in stratification affecting convection processes, which directly impact the Mediterranean thermohaline circulation and the climate system.

Data availability

907

908

909

910

\$11

912

913

914

\$15

916

\$17

918

\$19

\$20

\$21

\$22

923

924

\$25

926

927

928

\$29

\$30

931

932

933

934

935

936

937

938

939

943

944

- The data that support the findings of this study are publicly available under the following links: SeaExplorer glider from (https://data-selection.odatis-ocean.fr/coriolis/uri/p83112098), CCC-1000 moored time series (https://doi.org/10.17882/104746; Sanchez-Vidal et al., 2025a), LDC-500 and LDC-1000 moored time series (https://doi.org/10.17882/45980; Durrieu de Madron et al., 2024). The CTD and the ADCP data collected during the FARDWO-CCC1 Cruise are available at https://doi.org/10.17882/105499 (Sanchez-Vidal et al., 2025b).
- **Authors contributions**
- AS, DA, XD, and FB defined the research problem, the conceptualization of the study, and leaded the acquisition of the study data. MA-C carried out the data analysis and produced the figures and first draft of the manuscript. All coauthors discussed the analyses and contributed to the review and writing of the final paper.

Competing interests

The authors declare that they have no conflict of interest.

Acknowledgements

945

952

957

958

\$59

960

961

\$62

963

964

965

966

967

968

969

970

971

972

973

974

975

976

\$77

978 979

980

981

982

983

984

\$85

- 946 We are very grateful to the captain, crew, and the scientific team for their dedication and hard work during the FARDWO-
- 947 CCC1 Cruise at the R/V García del Cid, and to the technicians for their guidance and assistance. We wish to thank the Alseamar
- Alcen technicians for the glider deployment and piloting, and the data pre-processing. We also want to thank Pascal Conan
- 949 from OSU-Stamar (Stations Marines UPMC de Banyuls-sur-Mer) at the Sorbonne Université, as well as acknowledge the
- 950 MOOSE, the COAST-HF and the SOMLIT programs coordinated by CNRS-INSU and the Research Infrastructure ILICO
- 951 (CNRS-IFREMER) for providing data from the POEM and SOLA buoys and the Lacaze-Duthiers Canyon's mooring.

Financial support

- 953 This work has been supported by the FARDWO (PID2020-114322RB-I00) project funded by
- 954 MICIU/AEI/10.13039/501100011033, the Catalan Government Excellent Research Groups gran no. 2021 SGR 01195, and the
- \$55 ANR MELANGE (ANR-19-ASMA-0004) project. MAC wasis supported by a Margarita Salas postdoctoral grant (2022-2024)
- \$56 from the Spanish Ministry of Universities throughout part of the project. HF is supported by the AGAUR FI-SDUR fellowship
 - number 2023-FISDU-00233 by Secretaria d'Universitats i Recerca from the Catalan Government.

References

Allen, S. E., and Durrieu de Madron, X.: A review of the role of submarine canyons in deep-ocean exchange with the shelf. Ocean Sci. 5, 607-620, https://doi.org/10.5194/os-5-607-2009, 2009.

Amblas, D., Dowdeswell, J. A.: Physiographic influences on dense shelf-water cascading down the Antarctic continental slope. Earth-Sci. Rev. 185, 887-900, https://doi.org/10.1016/j.earscirev.2018.07.014, 2018.

Arjona-Camas, M., Puig, P., Palanques, A., Durán, R., White, M., Paradis, S., and Emelianov, M.: Natural vs. trawling-induced water turbidity and suspended sediment transport variability within the Palamós Canyon (NW Mediterranean). Mar. Geophys. Res. 42, 38, https://doi.org/10.1007/s11001-021-09457-7, 2021.

Béthoux, J., Durrieu de Madron, X., Nyffeler, F., and Taiiliez, D.: Deep water in the western Mediterranean: peculiar 1999 and 2000 characteristics, shelf formation hypothesis, variability since 1970 and geochemical interferences. J. Mar. Sys. 33, 117-131, http://doi.org/ 10.1016/S0924-7963(02)00055-6, 2002.

Blair, N. E., and Aller, R. C.: The fate of terrestrial organic carbon in the marine environment. Annu. Rev. Mar. Sci. 4, 401-423, https://doi.org/10.1146/annurev-marine-120709-142717, 2012.

Bourrin, F. and Durrieu de Madron, X.: Contribution to the study of coastal rivers and associated prodeltas to sediment supply in the Gulf of Lions (NW Mediterranean Sea). Life Environ. 56, 307-31, 2006.

Bourrin, F., Durrieu de Madron, X., Heussner, S., and Estournel, C.: Impact of winter dense water formation on shelf sediment erosion (evidence from the Gulf of Lions, NW Mediterranean). Cont. Shelf Res. 28, 1984-1999, https://doi.org/10.1016/j.csr.2008.06.006, 2008.

Bourrin, F., Many, G., Durrieu de Madron, X., Martín, J., Puig, P., Houpert, L., Testor, P., Kunesch, S., Mahiouz, K., and Béguery, L.: Glider monitoring of shelf suspended particle dynamics and transport during storm and flooding conditions. Cont. Shelf Res. 109, 135-149, https://doi.org/10.1016/j.csr.2015.08.031, 2015.

Bourrin, F., Zudaire, L., Vala, T., Vuillemin, R., Conan, P., and Kunesch, S.: POEM Coastal Buoy. SEANOE. https://doi.org/10.17882/88936, 2022.

Canals, M., Puig, P., Durrieu de Madron, X., Heussner, S., Palanques, A., and Fabres, J.: Flushing submarine canyons. Nature d444, 354-357, https://doi.org/10.1038/nature05271, 2006.

Cenedese, C., Whitehead, J. A., Ascarelli, T. A., and Ohiwa, M.: A dense water current flowing down a sloping bottom in a rotating fluid. J. Phys. Oceanogr. 34, 188-203, https://doi.org/10.1175/1520-0485(2004)034%3C0188:ADCFDA%3E2.0.CO;2, 2004.

992

997

998

999 1000 1001

1003 1004 1005

1002

1006 1007 1008

1009 1010 1011

1012 1013 1014

1015 1016 1017

1018 1019

1021 1022

1020

1023 1024 1025

1026

1027

1028

Chapron, L., Lebris, N., Durrieu de Madron, X., Peru, E., Galand, P., and Lartaud, F.: Long term monitoring of coldwater coral growth shows response to episodic meteorological events in the NW Mediterranean. Deep Sea Res. I Oceanogr. Pap. 160, 103255.

Conan, P., Maria, E., Labatut, P., Zudaire, L., Pujo-Pay, M., Pecqueur, D., Salmeron, C., Crispi, O., Marie, B., and Vuillemin, R.: SOMLIT-SOLA time series (French Research Infrastructure ILICO): long-term core parameter monitoring in the Bay of Banyuls-sur-Mer. SEANOE. https://doi.org/10.17882/99794, 2024.

Danoyaro, R., Gambi, C., Dell'Anno, A., Corinaldesi, C., Fraschetti, S., Vanreusel, A., Vincx, M., and Gooday, A.: Exponential decline of deep-sea ecosystem functioning linked to benthic ecosystem loss. Curr. Biol. 18, 1-18, https://doi.org/10.1016/j.cub.2007.11.056, 2008.

Davies, P. A., Dakin, J. M., and Falconer, R. A.: Eddy formation behind a coastal headland. J. Coast. Res. 1, 154-167, http://www.jstor.org/stable/4298318, 1995.

Davis, R. A., and Hayes, M. O.: What is a wave-dominated coast? Mar. Geol. 60, 313-319, https://doi.org/10.1016/0025-3227(84)90155-5, 1984.

DeGeest, A.L., Mullenbach, B. L., Puig, P., Nittrouer, C. A., Drexler, T. M., Durrieu de Madron, X., Orange, D. L.: Sediment accumulation in the western Gulf of Lions, France: the role of Cap de Creus Canyon in linking shelf and slope sediment dispersal systems. Cont. Shelf Res. 28, 2031-2047, https://doi.org/10.1016/j.csr.2008.02.008, 2008.

Dipper, F.: The seawater environment and ecological adaptations, in: Elements of Marine Ecology (Fifth Edition), edited by: Butterworth-Heinemann, Oxford, UK, 37-151, https://doi.org/10.1016/B978-0-08-102826-1.00002-8, 2022.

Drexler, T. M., and Nittrouer, C. A.: Stratigraphic signatures due to flood deposition near the Rhône River: Gulf of Lions, northwest Mediterranean Sea. Cont. Shelf Res. 28, 1877-1894, https://doi.org/10.1016/j.csr.2007.11.012, 2008.

Dufau-Julliand, C., Marsaleix, P., Petrenko, A., and Dekeyser, I.: Three-dimensional modeling of the Gulf of Lion's hydrodynamics (northwest Mediterranean) during January 1999 (MOOGLI3 Experiment) and late winter 1999: Western Mediterranean Intermediate Water's (WIW's) formation and its cascading over the shelf break. J. Geophys. Res. Oceans, 109, https://doi.org/10.1029/2003JC002019, 2004.

Durán, R., Canals, M., Sanz, J. L., Lastras, G., Amblas, D., and Micallef, A.: Morphology and sediment dynamics of the northern Catalan continental shelf, northwestern Mediterranean Sea. Geomorphology, 204, 1-20, https://doi.org/10.1016/j.geomorph.2012.10.004, 2014.

Durrieu de Madron, X., Nyffeler, F., and Godet, C. H.: Hydrographic structure and nepheloid spatial distribution in the Gulf of Lions continental margin. Cont. Shelf Res. 10, 915-929, https://doi.org/10.1016/0278-4343(90)90067-V, 1990.

Durrieu de Madron, X. and Panouse, M.: Transport de matière en suspension sur le plateau continental du Golfe de Lion-Situation estivale et hivernale. Comptes Rendus de l'Académie des Sciences, Série Ila, Paris, 322, 1061-1070, 1996.

Durrieu de Madron, X., Zervakis, V., Therocharis, A., and Georgopoulos, D.: Comments on "Cascades of dense water around the world ocean". Prog. Oceanogr. 64, 83-90, https://doi.org/10.1016/j.pocean.2004.08.004, 2005.

Durrieu de Madron, X., Wiberg, P. L., and Puig, P. Sediment dynamics in the Gulf of Lions: The impact of extreme events. Cont. Shelf Res. 28, 1867-1876, https://doi.org/10.1016/j.csr.2008.08.001, 2008.

Durrieu de Madron, X., Houpert, L., Puig, P., Sanchez-Vidal, A., Testor, P., Bosse, A., Estournel, C., Somot, S., Bourrin, F., Bouin, M. N., Beauverger, M., Beguery, L., Canals, M., Cassou, C., Coppola, L., Dausse, F., D'Ortenzio, F., Font, J., Heussner, S., Kunesch, S., Lefevre, D., Le Goff, H., Martín, J., Mortier, L., Palanques, A., and Raimbault, P.: Interaction of dense shelf water cascading and open-sea convection in the northwestern Mediterranean during winter 2012. Geophys. Res. Lett. 40, 1379-1385, https://doi.org/10.1002/grl.50331, 2013.

Durrieu de Madron, X., Aubert, D., Charrière, B., Kunesch, S., Menniti, C., Radakovitch, O., and Sola, J.: Impact of dense water formation on the transfer of particles and trace metals from the coast to the deep in the northwestern Mediterranean. Water, 15, 301, https://doi.org/10.3390/w15020301, 2023.

Durrieu de Madron, X., Heussner, S., Delsaut, N., Stéphane, K., Menniti, C.: BILLION observatory data. SEANOE. https://doi.org/10.17882/45980, 2024.

1031

1032

1033

1034

1035

1036

1037

1038

1039

1**0**40 1041

1042

1043

1044

1045

1046

1047

1048

1049

1050

1**0**51

1052

1053

1054

1055

1056

1057

1058

1059

1060

1061

1062

1063

1064

1**¢**65

1066

1067

1**0**68

1069

Escudier, R., Clementi, E., Omar, M., Cipollone, A., Pistoia, J., Aydogdu, A., Drudi, M., Grandi, A., Lyubartsev, V., Lecci, R., Cretí, S., Masina, S., Coppini, G., and Pinardi, N.: Mediterranean Sea Physical Reanalysis (CMEMS MED-Currents) (Version 1) [Data set]. Copernicus Monitoring Environment Marine Service (CMEMS), https://doi.org/10.25423/CMCC/MEDSEA MULTIYEAR PHY 006 004 E3R1, 2020.

Escudier, R., Clementi, E., Cipollone, A., Pistoia, J., Drudi, M., Grandi, A., Luybartsev, V., Lecci, R., Aydogdu, A., Delrosso, D., Omar, M., Masina, S., Coppini, G., and Pinardi, N.: A high resolution reanalysis for the Mediterranean Sea. Front. Earth Sci. 9, 702285, https://doi.org/10.3389/feart.2021.702285, 2021.

Estournel, C., Durrieu de Madron, X., Marsaleix, P., Auclair, F., Julliand, C., and Vehil, R.: Observation and modeling of the winter coastal oceanic circulation in the Gulf of Lion under wind conditions influenced by the continental orography (FETCH experiment). J. Geophys. Res. Oceans, 108, https://doi.org/10.1029/2001JC000825, 2003.

Estournel, C., Mikolajczak, G., Ulses, C., Bourrin, F., Canals, M., Charmasson, S., Doxaran, D., Duhaut, T., Durrieu de Madron, D., Marsaleix, P., Palanques, A., Puig, P., Radakovitch, O., Sanchez-Vidal, A., and Verney, R.: Sediment dynamics in the Gulf of Lion (NW Mediterranean Sea) during two autumn–winter periods with contrasting meteorological conditions. Prog. Oceanogr. 210, 102942, https://doi.org/10.1016/j.pocean.2022.102942, 2023.

Fabres, J., Tesi, T., Velez, J., Batista, F., Lee, C., Calafat, A., Heussner, S., Palanques, A., and Miserocchi, S.: Seasonal and event-controlled export of organic matter from the shelf towards the Gulf of Lions continental slope. Cont. Shelf Res. 28, 1971-1983, https://doi.org/10.1016/j.csr.2008.04.010, 2008.

Feistel, R.: A new extended Gibbs thermodynamic potential of seawater. Prog. Oceanogr. 58, 43-114, https://doi.org/10.1016/S0079-6611(03)00088-0, 2003.

Feistel, R.: A Gibbs function for seawater thermodynamics for -6 to 80 C and salinity up to 120 g·kg⁻¹. Deep Sea Res. I-Oceans, 55, 1639-1671, https://doi.org/10.1016/j.dsr.2008.07.004, 2008.

Ferré, B., Durrieu de Madron, X., Estournel, C., Ulses, C., and Le Corre, G.: Impact of natural (waves and currents) and anthropogenic (trawl) resuspension on the export of particulate matter to the open ocean: application to the Gulf of Lion (NW Mediterranean). Cont. Shelf Res. 28, 2071-2091, https://doi.org/10.1016/j.csr.2008.02.002, 2008.

Fischer, J., and Visbeck, M.: Deep Velocity Profiling with Self-contained ADCPs. J. Atmos. Ocean. Technol. 10, 764-773, https://doi.org/10.1175/1520-0426(1993)010%3C0764:DVPWSC%3E2.0.CO;2, 1993.

Font, J.: The path of the Levantine intermediate water to the Alboran Sea. Deep Sea Res. I Oceanogr. Res. Pap. 34, 1745-1755, https://doi.org/10.1016/0198-0149(87)90022-7, 1987.

Font, J., Puig, P., Salat, J., Palanques, A., and Emelianov, M.: Sequence of hydrographic changes in the NW Mediterranean deep water due to the exceptional winter of 2005. Sci. Mar. 71, 339-346, https://doi.org/10.3989/scimar.2007.71n2339, 2007.

Fos, H., Izquierdo-Peña, J., Amblas, D., Arjona-Camas, M., Romero, L., Estella-Pérez, V., Florindo-Lopez, C., Calafat, A., Cerdà-Domènech, M., Puig, P., Durrieu de Madron, X., and Sanchez-Vidal, A.: Solving dense shelf water cascading with a high-resolution ocean reanalysis. ESS Open Archive, March 17, https://doi.org/10.22541/essoar.174060515.57729804/v2, 2025.

Fugate, D.C., and Friedrichs, C.T.: Determining concentration and fall velocity of estuarine particle populations using ADV, OBS and LISST. Cont. Shelf Res. 22 (11–13), 1867–1886, https://doi.org/10.1016/S0278-4343(02)00043-2, 2002.

Gales, J., Rebesco, M., De Santis, L., Bergamasco, A., Colleoni, F., Kim S., Accetella, A., Kovacevic, V., Liu, Y., Olivo, E., Colizza, E., Florindo-Lopez, C., Zgur, F., McKay, R.: Role of dense shelf water in the development of Antarctic submarine canyon morphology. Geomorphology, 372, 107453, https://doi.org/10.1016/j.geomorph.2020.107453, 2021.

Gartner, J. W.: Estimating suspended soils concentrations from backscatter intensity measured by acoustic Doppler current profiler in San Francisco Bay, California. Mar. Geol. 211, 169-187, https://doi.org/10.1016/j.margeo.2004.07.001, 2004.

1φ85

096

1φ97

Guillén, J., Bourrin, F., Palanques, A., Durrieu de Madron, X., Puig, P., and Buscail, R.: Sediment dynamics during 'wet' and 'dry' storm events on the Têt inner shelf (SW Gulf of Lions). Mar. Geol. 234, 129-142, https://doi.org/10.1016/j.margeo.2006.09.018, 2006.

Guizien, H.: Spatial variability of wave conditions in the Gulf of Lions (NW Mediterranean Sea). Vie et Milieu/Life & Environment, 261-270, 2009.

Herrmann, M., Estournel, C., Déqué, M., Marsaleix, P., Sevault, F., and Somot, S.: Dense water formation in the Gulf of Lions shelf: Impact of atmospheric interannual variability and climate change. Cont. Shelf Res. 28, 2092-2112, https://doi.org/10.1016/j.csr.2008.03.003, 2008.

Hersbach, H., Bell, B., Berrisford, P., Biavati, G., Horányi, A., Muñoz Sabater, J., Nicolas, J., Peubey, C., Radu, R., Rozum, I., Schepers, D., Simmons, A., Soci, C., Dee, D., and Thépaut, J-N. ERA5 hourly data on pressure levels from 1940 to present. Copernicus Climate Change Service (C3S) Climate Data Store (CDS). https://doi.org/10.24381/cds.bd0915c6, 20242023.

Heussner, S., Durrieu de Madron, X., Calafat, A., Canals, M., Carbonne, J., Desault, N., and Saragoni, G.: Spatial and temporal variability of downward particle fluxes on a continental slope: lessons from an 8-yr experiment in the Gulf of Lions (NW Mediterranean). Mar. Geol. 234, 63-92, https://doi.org/10.1016/j.margeo.2006.09.003, 2006.

Homrani, S., de Fommervault, P., Gentil, M., Jourdin, F., Durrieu de Madron, X., Bourrin, F.: Tracing suspended sediment fluxes using a glider: observations in a tidal shelf environment. EGUsphere, 1-35, https://doi.org/10.5194/egusphere-2024-4072, 2025.

Houpert, L., Durrieu de Madron, X., Testor, P., Bosse, A., D'Ortenzio, F., Bouin, M. N., Dausse, D., Le Goff, H., Kunesch, S., Labaste, M., Coppola, L., Mortier, L., and Raimbault, P.: Observations of open-ocean deep convection in the northwestern Mediterranean Sea: Seasonal and interannual variability of mixing and deep water masses for the 2007-2013 Period. J. Geophys. Res. Oceans, 121, 8139-8171, https://doi.org/10.1002/2016JC011857, 2016.

Ivanov, V. V., Shapiro, G. I., Huthnance, J. M., Aleynik, D. L., and Golovin, P. N.: Cascades of dense water around the world. Progr. Oceanogr. 60, 47-98. https://doi.org/10.1016/j.pocean.2003.12.002, 2004.

Kwon, E., DeVries, T., Galbraith, E. D., Hwang, J., Kim, G., and Timmermann, A.: Stable carbon isotopes suggest large terrestrial carbon inputs to the global ocean. Global Biogeochem. Cycles 35: e2020GB006684, https://doi.org/10.1029/2020GB006684, 2021.

Juza, M., Renault, L., Ruiz, S., and Tintoré, J.: Origin and pathways of Winter Intermediate Water in the Northwestern Mediterranean Sea using observations and numerical simulation. J. Geophys. Res. 118, 6621-6633, https://doi.org/10.1002/2013JC009231, 2013.

Juza, M., Escudier, R., Vargas-Yáñwz, M., Mourre, B., Heslop, E., Allen, J., and Tintoré, J.: Characterization of changes in Western Intermediate Water properties enabled by an innovative geometry-based detection approach. J. Mar. Sys. 191, 1-12, https://doi.org/10.1016/j.jmarsys.2018.11.003, 2019.

Lastras, G., Canals, M., Urgeles, R., Amblas, D., Ivanov, M., Droz, L., Dennielou, B., Fabrés, J., Schoolmeester, T., Akhmetzhanov, A., Orange, D., and García-García, A.: A walk down the Cap de Creus Canyon, Northwestern Mediterranean Sea: Recent processes inferred from morphology and sediment bedforms. Mar. Geol. 246, 176-192, https://doi.org/10.1016/j.margeo.2007.09.002, 2007.

Lapouyade A. and Durrieu de Madron, X.: Seasonal variability of the advective transport of particulate and organic carbon in the Gulf of Lion (NW Mediterranean). Oceanol. Acta, 24, 295-312, https://doi.org/10.1016/S0399-1784(01)01148-3, 2001.

- Le Bot, P., Kermabon, C., Lherminier, P., and Gaillard, F.: CASCADE V6.1: Logiciel de validation et de visualisation des mesures ADCP de coque. Rapport technique OPS/LPO 11-01. Ifremer, Centre de Brest, France, 2011.
- Leredde, Y., Denamiel, C., Brambilla, E., Lauer-Leredde, C., Bouchette, F., and Marsaleix, P.: Hydodynamics in the
 Gulf of Aigues-Mortes, NW Mediterranean Sea: In situ and modelling data. Cont. Shelf Res. 27, 2389-2406,
 https://doi.org/10.1016/j.csr.2007.06.006, 2007.
- Levin, L. A. and Sibuet, M.: Understanding continental margin biodiversity: a new imperative. Annu. Rev. Mar. Sci. 4, 79-112, http://doi.org/10.1146/annurev-marine-120709-142714, 2012.
- Liu, Z., Zhao, Y., Colin, C., Stattegger, K., Wiesner, M. G., Huh, C. A., Zhang, Y., Li, X., Sompongchaiyakul, P., You, C. F., Huany, C., Liu, J. T., Siringan, F. P., Le, Sathiamurthy, E., Hantoro, W. S., Liu, J., Tuo, S., Zhao, S., Zhou, S., He,

128

- Z., Wang, Y., Bunsomboonsakul, S., and Li, Y.: Source-to-sink transport processes of fluvial sediments in the South China Sea. Earth Sci. Rev. 153, 238-273, https://doi.org/10.1016/j.earscirev.2015.08.005, 2016.
 - Lohrmann, A.: Monitoring Sediment Concentration with Acoustic Backscattering Instruments. Nortek, 2001.
- Ludwig, W., Dumont, E., Meybeck, M., and Heussner, S.: River discharges of water and nutrients to the Mediterranean and Black Sea: major drivers for ecosystem changes during past and future decades? Prog. Oceanogr. 80, 199-217, https://doi.org/10.1016/j.pocean.2009.02.001, 2009.
- Mack, S. A., and Schoeberlein, H. C.: Richardson number and ocean mixing: towed chain observations. J. Phys. Oceanogr. 34, 736-754, https://doi.org/10.1175/1520-0485(2004)034<0736:RNAOMT>2.0.CO;2, 2004.
- Mahjabin, T., Pattiaratchi, C., Hetzel, Y., and Janekovic, I.: Spatial and temporal variability of dense shelf water cascades along the Rottnest continental shelf in southwest Australia. J. Mar. Sci. Eng. 7, 30, https://doi.org/10.3390/jmse7020030, 2019.
- Mahjabin, T., Pattiaratchi, C., and Hetzel, Y.: Occurrence and seasonal variability of Dense Shelf Water Cascades along Australian continental shelves. Sci. Rep. 10, 9732, https://doi.org/10.1038/s41598-020-66711-5, 2020.
- Margirier, F., Testor, P., Heslop, E., Mallil, K., Bosse, A., Houpert, L., Mortier, L., Bouin, M., Coppola, L., D'Ortenzio, F., Durrieu de Madron, X., Mourre, B., Prieur, L., Raimbault, P., and Taillandier, V.: Abrupt warming and salinification of intermediate waters interplays with decline of deep convection in the Northwestern Mediterranean Sea. Sci. Rep. 10, 20923, https://doi.org/10.1038/s41598-020-77859-5, 2020.
- Martín, J., Durrieu de Madron, X., Puig, P., Bourrin, F., Palanques, A., Houpert, L., Higueras, M., Sánchez-Vidal, A., Calafat, A. M., Canals, M., Heussner, S., Delsaut, N., and Sotin, C.: Sediment transport along the Cap de Creus canyon flank during a mild, wet winter. Biogeosciences 10(5):3221-3239, https://doi.org/10.5194/bg-10-3221-2013, 2013.
- Marshall, J., and Schott, F.: Open-ocean convection: Observations, theory, and models. Rev. Geophys. 37, 1-64, https://doi.org/10.1029/98RG02739, 1999.
- Mendoza, E. T. and Jiménez, A. A.: Vulnerability assessment to coastal storms at a regional scale. In: Coastal engineering 2008, vol. 5, pp. 4154-4166, https://doi.org/10.1142/9789814277426_0345, 2009.
- Mikolajczak, G., Estournel, C., Ulses, C., Marsaleix, P., Bourrin, F., Martín, J., Pairaud, I., Puig, P., Leredde, Y., Many, G., Seyfried, L., and Durrieu de Madron, X.: Impact of storms on residence times and export of coastal waters during a mild autumn/winter period in the Gulf of Lion. Cont. Shelf Res. 207, 104192, https://doi.org/10.1016/j.csr.2020.104192, 2020.
- 1151 Millot, C.: The Gulf of Lions' hydrodynamics. Cont. Shelf Res. 10, 885-894, https://doi.org/10.1016/0278-1152 4343(90)90065-T, 1990.
 - Millot, C.: Circulation in the Western Mediterranean. J. Mar. Syst. 20, 423-442, https://doi.org/10.1016/S0924-7963(98)00078-5, 1999.
 - Monin, A., and Yaglom, A.: Statistical Fluid Mechanics, vol. 1, The MIT Press, Cambridge, Massachusetts and London, England, 1971.

Nittrouer, C. A., Austin, J. A., Field, M. E., Kravitz, J. H., Syvitski, J. P., and Wiberg, P. L.: Continental margin sedimentation: from sediment transport to sequence stratigraphy, John Wiley and Sons (Eds), http://doi.org/10.1002/9781444304398, 2009.

Odic, R., Bensoussan, N., Pinazo, C., Taupier-Letage, I., and Rossi, V.: Sporadic wind-driven upwelling/downwelling and associated cooling/warming along Northwestern Mediterranean coastlines. Cont. Shelf Res. 250, 104843, https://doi.org/10.1016/j.csr.2022.104843, 2022.

Ogston, A. S., Drexler, T. M., and Puig, P.: Sediment delivery, resuspension, and transport in two contrasting canyon environments in the southwest Gulf of Lions. Cont. Shelf Res. 28, 2000-2016, https://doi.org/10.1016/j.csr.2008.02.012, 2008.

Palanques, A., Durrieu de Madron, X., Puig, P., Fabrés, J., Guillén, J., Calafat, A., Canals, M., Heussner, S., and Bonnin, J.: Suspended sediment fluxes in the Gulf of Lions submarine canyons. The role of storms and dense water cascading. Mar. Geol. 234, 43-61, https://doi.org/10.1016/j.margeo.2006.09.002, 2006.

Palanques, A., Guillén, J., Puig, P., and Durrieu de Madron, X.: Storm-driven shelf-to-canyon suspended sediment transport at the southwestern Gulf of Lions. Cont. Shelf Res. 28, 1947-1956, https://doi.org/10.1016/j.csr.2008.03.020, 2008.

Palanques, A., Puig, P., Latasa, M., and Scharek, R.: Deep sediment transport induced by storms and dense shelf-water cascading in the northwestern Mediterranean basin. Deep Sea Res. Pt I. 56, 425 434, https://doi.org/10.1016/j.dsr.2008.11.002, 2009.

Palanques, A., Puig, P., Durrieu de Madron, X., Sanchez-Vidal, A., Pasqual, C., Martín, J., Calafat, A., Heussner, S., and Canals, M.: Sediment transport to the deep canyons and open-slope of the western Gulf of Lions during the 2006 intense cascading and open-sea convection period. Prog. Oceanogr. 106, 1-15, https://doi.org/10.1016/j.pocean.2012.05.002, 2012.

Palanques, A., and Puig, P.: Particle fluxes induced by benthic storms during the 2012 dense shelf water cascading and open sea convection period in the northwestern Mediterranean Basin. Mar. Geol. 406, 119-131, https://doi.org/10.1016/j.margeo.2018.09.010, 2018.

Parras-Berrocal, I. M., Vázquez, R., Cabos, W., Sein, D. V., Álvarez, O., Bruno, M., and Izquierdo, A.: Surface and intermediate water changes triggering the future collapse of deep water formation in the North Western Mediterranean. Geophys. Res. Lett. 49, e2021GL095404, https://doi.org/10.1029/2021GL095404, 2022.

Pasqual, C., Sanchez-Vidal, A., Zúñiga, D., Calafat, A., Canals, M., Durrieu de Madron, X., Puig, P., Palanques, A., and Delsaut, N.: Flux and composition of settling particles across the continental margin of the Gulf of Lion: the role of dense shelf water cascading. Biogeosciences, 7, 217-231, https://doi.org/10.5194/bg-7-217-2010, 2010.

Petrenko, A.: Variability of circulation features in the Gulf of Lion, NW Mediterranean Sea. Importance of inertial currents.

Oceanol. Acta 26: 323–338, https://doi.org/10.1016/S0399-1784(03)00038-0, 2008.

Petrenko, A., Dufau, C., and Estournel, C.: Barotropic eastward currents in the western Gulf of Lion, north-western Mediterranean Sea, during stratified conditions. J. Mar. Syst. 74, 406-428, https://doi.org/10.1016/j.jmarsys.2008.03.004, 2008.

Pont, D., Simonnet, J. P., and Walter, A. V.: Medium-term changes in suspended sediment delivery to the ocean: consequences of catchment heterogeneity and river management (Rhône River, France). Estuar. Coast. Shelf Sci. 54, 1-18, http://doi.org/10.1006/ecss.2001.0829, 2002.

Pörtner, H. O. and Knust, R.: Climate change affects marine fishes through oxygen limitation of thermal tolerance. Science, 315, 95-97, https://doi.org/10.1126/science.1135471, 2007.

Poulier, G., Launay, M., Le Bescond, C., Thollet, F., Coquery, M., and Le Coz, J.: Combining flux monitoring and data reconstruction to establish annual budgets of suspended particulate matter, mercury and PCB in the Rhône River from Lake Geneva to the Mediterranean Sea. Sci. Total Environ. 658, 457-273, https://doi.org/10.1016/j.scitotenv.2018.12.075, 2019.

Provansal, M., Dufour, S., Sabatier, F., Anthony, E. J., Raccasi, G., and Robresco, S.: The geomorphic evolution and sediment balance of the lower Rhône River (southern France) over the last 130 years: Hydropower dams versus other control factors. Geomorphology, 219, 27-41, https://doi.org/10.1016/j.geomorph.2014.04.033, 2014.

Puig, P.: Dense shelf water cascading and associated beforms. In: Guillén, J., Acosta, J., Chiocci, F., and Palanques, A. (eds). Atlas of Bedforms in the Western Mediterranean. Springer, Cham. https://doi.org/10.1007/978-3-319-33940-5_7, 2017.

Puig, P., Company, J. B., Sardà, F., and Palanques, P.: Responses of deep-water shrimp populations to intermediate nepheloid layer detachments on the Northwestern Mediterranean continental margin. Deep Sea Res. I Oceanogr. Res. Pap. 48, 2195-2207, https://doi.org/10.1016/S0967-0637(01)00016-4, 2001.

Puig, P., Palanques, A., Orange, D. L., Lastras, G., and Canals, M.: Dense shelf water cascades and sedimentary furrow formation in the Cap de Creus Canyon, northwestern Mediterranean Sea. Cont. Shelf Res. 28, 2017-2030, https://doi.org/10.1016/j.csr.2008.05.002, 2008.

Puig, P., Palanques, A., and Martín, J.: Contemporary sediment-transport in submarine canyons. Annu. Rev. Mar. Sci. 6, 53-77, https://doi.org/10.1146/annurev-marine-010213-135037, 2014.

Pusceddu, A., Mea, M., Canals, M., Heussner, S., Durrieu de Madron, X., Sanchez-Vidal, A., Bianchelli, S., Corinaldesi, A., Dell'Anno, A., Thomsen, L., and Danovaro, R.: Major consequences of an intense dense shelf water cascading event on deep-sea benthic trophic conditions and meiofaunal biodiversity. Biogeosciences 10, 2659-2670, https://doi.org/10.5194/bg-10-2659-2013, 2013.

Raimbault, P., and Durrieu de Madron, X.: Research activities in the Gulf of Lion (NW Mediterranean) within the 1997 2001 PNEC Project. Oceanol. Acta 26, 291–298, https://doi.org/10.1016/S0399-1784(03)00030-6, 2003.

Ribó, M., Puig, P., Palanques, A., and Lo Iacono, C.: Dense shelf water cascades in the Cap de Creus and Palamós submarine canyons during winters 2007 and 2008. Mar. Geol. 284, 175-188, https://doi.org/10.1016/j.margeo.2011.04.001,

2011.

Rumín-Caparrós, A., Sanchez-Vidal, A., Calafat, A. M., Canals, M., Martín, J., Puig, P., and Pedrosa-Pàmies, R.:

External forcings, oceanographic processes and particle flux dynamics in Cap de Creus submarine canyon, NW Mediterranean. Biogeosciences Discussions 9(12), https://digital.csic.es/handle/10261/78113, 2013.

Sadaoui, M., Ludwig, W., Bourrin, F., and Raimbault, P.: Controls, Budgets and Variability of Riverine Sediment Fluxes to the Gulf of Lions (NW Mediterranean Sea). J. Hydrol. 540, 1002–1015, https://doi.org/10.1016/j.jhydrol.2016.07.012, 2016.

Sanchez-Vidal, A., Pasqual, C., Kerhervé, P., Heussner, S., Palanques, A., Durrieu de Madron, X., Canals, M., and Puig, P.: Impact of dense shelf water cascading on the transfer of organic matter to the deep western Mediterranean basin. Geophys. Res. Lett. 35, https://doi.org/10.1029/2007GL032825, 2008.

Sanchez-Vidal, A., Calafat, A., Amblas, D., Cerdà-Domènech, M., Fos, H.: CC1000 observatory data. SEANOE. https://doi.org/10.17882/105504, 2025a.

Sanchez-Vidal, A., Amblas, D., Arjona-Camas, M., Durrieu de Madron, X., Calafat, A., Cerdà-Domènech, M., Pena, L.D., Espinosa, S.: CTD and ADCP data collected during the cruise FARDWO CC1. SEANOE. http://doi.org/10.17882/105499, 2025b.

Schlitzer, R.: Ocean Data View. https://odv.awi.de/, 2023.

Schroeder, K., Josey, S. A., Herrmann, M., Grignon, L., Gasparini, G. P., and Bryden, H. L.: Abrupt warming and salting of the Western Mediterranean Deep Water: Atmospheric forcings and lateral advection. J. Geophys. Res., 115, C08029, https://doi.org/10.1029/2009JC005749, 2010.

Schroeder, K., Ben Ismail, S., Bensi, M., Bosse, A., Chiggiato, K., Civitarese, G., Falcieri M, F., Fusco, G., Gacic, M., Gertman, I., Kubin, E., Malanotte-Rizzoli, P., Martellucci, R., Menna, M., Ozer, T., Taupier-Letage, I., Vargas-Yañez,

M., Velaoras, D. and Vilibic, I.: A consensus-based, revised and comprehensive catalogue for Mediterranean water masses acronyms. *Mediterranean Marine Science*, 25(3), 783–791, https://doi.org/10.12681/mms.38736, 2024.

- Serrat, P., Ludwig, W., Navarro, B., and Blazi, J. L.: Variabilité spatio-temporelle des flux de matières en suspension d'un fleuve côtier méditerranéen: la Têt (France). Comptes Rendus de l'Académie des Sciences-Series IIA-Earth and Planetary Science, 333(7), 389-397, https://doi.org/10.1016/S1251-8050(01)01652-4, 2001.
 - Shapiro, G. I., and Hill, A. E.: The alternative density structures of cold/saltwater pools on a sloping bottom: the role of friction. J. Phys. Oceanogr. 33, 390-406, https://doi.org/10.1175/1520-0485(2003)033<0390:TADSOC>2.0.CO;2, 2003.
 - Smith, M. D., Knapp, A. K., and Collins, S. L.: A framework for assessing ecosystem dynamics in response to chronic resource alterations induced by global change. Ecology, 90, 3279-3289, https://doi.org/10.1890/08-1815.1, 2009.
 - Somot, S., Sevault, F., and Déqué, M.: Transient climate change scenario simulation of the Mediterranean Sea for the twenty-first century using a high-resolution ocean circulation model. Clim. Dynam. 27, 851-879, https://doi.org/10.1007/s00382-006-0167-z, 2006.
 - Somot, S., Houpert, L., Sevault, F., Testor, P., Bosse, A., Taupier-Letage, I., Bouin, M. N., Waldman, R., Cassou, C., Sanchez-Gomez, E., Durrieu de Madron, X., Adloff, F., Nabat, P., and Herrmann, M.: Characterizing, modelling and understanding the climate variability of the deep water formation in the North-Western Mediterranean Sea. Clim. Dynam. 51, 1179-1210, https://doi.org/10.1007/s00382-016-3295-0, 2016.
 - Taillandier, V., D'Ortenzio, F., Prieur, L., Conan, P., Coppola, L., Cornec, M., Dumas, F., Durrieu de Madron, X., Fach, B., Fourrier, M., Gentil, M., Hayes, D., and Husrevoglu, S.: Sources of the Levantine Intermediate Water in winter 2019. J. Geophys. Res. Oceans, 127, e2021JC017506, https://doi.org/10.1029/2021JC017506, 2022.
 - Tesi, T., Puig, P., Palanques, A., and Goñi, M.: Lateral advection of organic matter in cascading-dominated submarine canyons. Prog. Oceanogr. 84, 185-203, https://doi.org/10.1016/j.pocean.2009.10.004, 2010.
 - Testor, P., Bosse, A., Houpert, L., Margirier, F., Mortier, L., Le Goff, H., Dausse, D., Labaste, M., Kartensen, J., Hayes, D., Olita, A., Ribotti, A., Schroeder, K., Chiggiato, J., Onken, R., Heslop, E., Mourre, B., D'Ortenzio, F., Mayot, N., Lavigne, H., Durrieu de Madron, X., Bourrin, F., Many, G., Damien, P., Estournel, C., Marsaleix, P., Taupier-Letage, I., Raimbault, P., Waldman, R., Bouin, M. N., Giordani, H., Caniaux, G., Somot, S., Ducrocq, V., and Conan, P.: Multiscale observations of deep convection in the northwestern Mediterranean Sea during winter 2012-2013 using multiple platforms. J. Geophys. Res. Oceans, 123, 1745-1776, https://doi.org/10.1002/2016JC012671, 2018.
 - Thurnherr, A. M., Symonds, D., and Laurent, L. S.: Processing explorer ADCP data collected on slocum gliders using the LADCP shear method. In Proceedings of the 2015 IEEEOES 11th Current Waves and Turbulence Measurement CWTM. St. Petersburg, FL, USA 2-6 March 2015, https://doi.org/10.1109/CWTM.2015.7098134, 2015.
 - Tubau, X., Lastras, G., Canals, M., Micallef, A., and Amblas, D.: Significance of the drainage pattern for submarine canyon evolution: The Foix Canyon System, Northwestern Mediterranean Sea. Geomorphology, 184, 20-37, https://doi.org/10.1016/j.geomorph.2012.11.007, 2013.
 - Ulses, C., Estournel, C., Bonnin, J., Durrieu de Madron, X., and Marsaleix, P.: Impact of storms and dense water cascading on shelf-slope exchanges in the Gulf of Lion (NW Mediterranean). J. Geophys. Res. Oceans, 113, http://doi.org/10.1029/2006JC003795, 2008a.
 - Ulses, C., Estournel, C., Puig, P., Durrieu de Madron, X., and Marsaleix, P.: Dense shelf water cascading in the northwestern Mediterranean during the cold winter 2005: Quantification of the export through the Gulf of Lion and the Catalan margin. Geophys. Res. Lett. 35(7), https://doi.org/10.1029/2008GL033257, 2008b.
 - Visbeck, M.: Deep velocity profiling using lowered acoustic Doppler current profilers: Bottom track and inverse solutions. J. Atmos. Oceanic Technol. 19, 794-807, https://doi.org/10.1175/1520-0426(2002)019%3C0794:DVPULA%3E2.0.CO;2, 2002.

1286	Walsh, J. P., and Nittrouer, C. A.: Understanding fine-grained river-sediment dispersal on continental margins. Mar
1287	Geol. 263, 34-45, https://doi.org/10.1016/j.margeo.2009.03.016, 2009.
1288	Wilson, G. W., and Hay, A. E.: Acoustic backscatter inversion for suspended sediment concentration and size: a new
1289	approach using statistical inverse theory. Cont. Shelf Res. 106, 130-139, https://doi.org/10.1016/j.csr.2015.07.005, 2015.

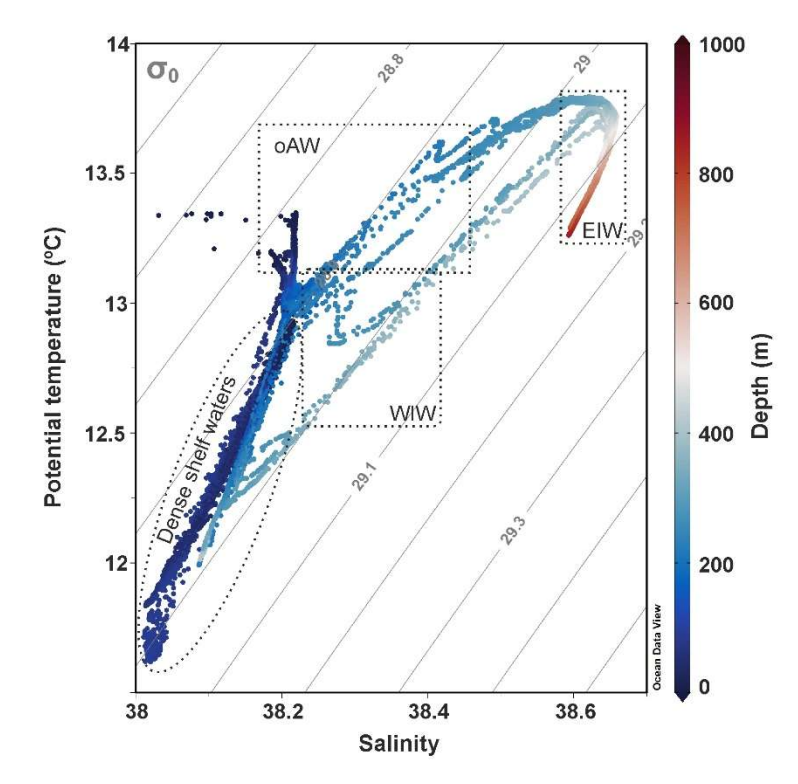


Figure A1. TS diagram from the CTD profiles collected during FARDWO-CCC1 T1 and T2 transects across the Cap de Creus Canyon, as well as those collected during the glider survey at the adjacent shelf (see Fig. 1b for positions). The different water masses that can be identified in the study area are: dense shelf waters, oAW (old Atlantic Water), WIW (Western Intermediate Water), and EIW (Eastern Intermediate Water).

Appendix B – Seasonality of chlorophyll-a between October 2021 and April 2022 from in situ measurements at the SOLA station.



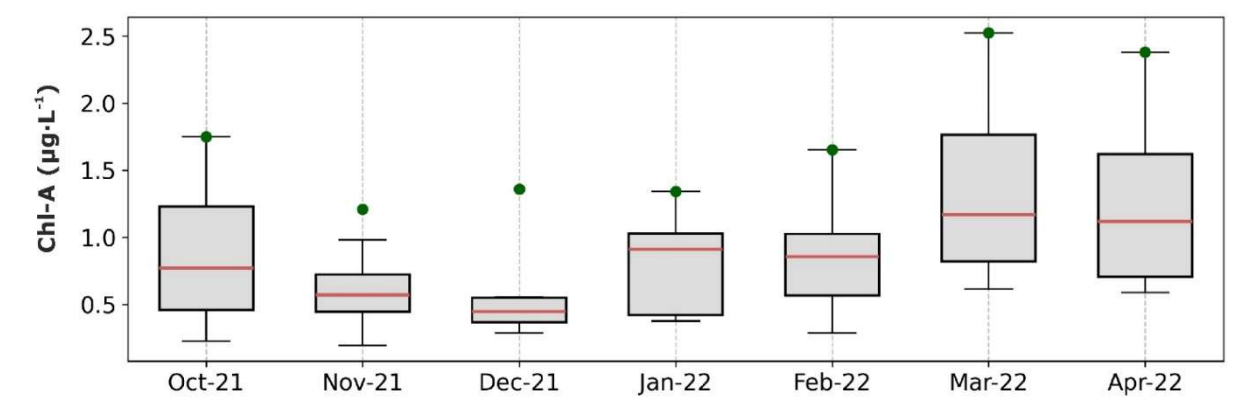


Figure B1. Seasonality of the chlorophyll-a measured at SOLA station between October 2021 and April 2022. Green dots indicate the monthly maximum values. Data has been retrieved from the SOMLIT-SOLA monitoring site in the Bay of Banyuls-sur-Mer (https://www.seanoe.org/data/00886/99794/; Conan et al., 2024).



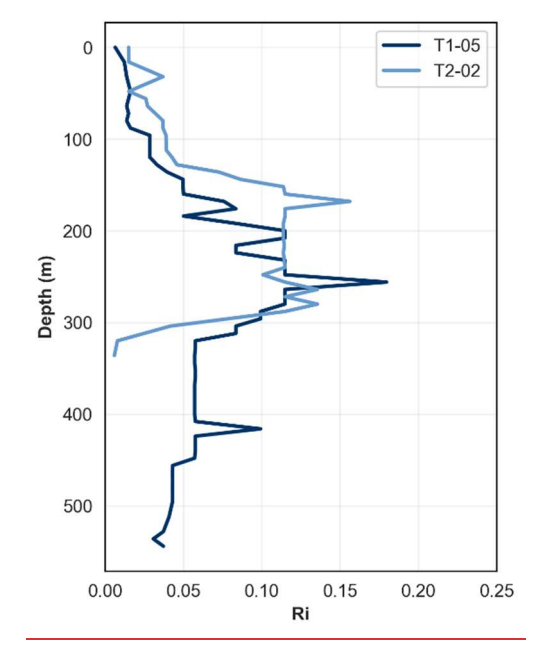


Figure C1. Vertical profiles of the Richardson number (Ri) calculated from CTD and LADCP measurements at two locations at the Cap de Creus Canyon where dense water were observed: T1-05 (upper canyon transect, dark blue) and T2-03 (mid-canyon transect, light blue). Values Ri <1 indicate a turbulent regime.